

**Britt T. McKinney**  
Sr. Vice President & Chief Nuclear Officer

**PPL Susquehanna, LLC**  
769 Salem Boulevard  
Berwick, PA 18603  
Tel. 570.542.3149 Fax 570.542.1504  
btmckinney@pplweb.com

JUN 27 2007



U. S. Nuclear Regulatory Commission  
Attn: Document Control Desk  
Mail Stop OP1-17  
Washington, DC 20555

**SUSQUEHANNA STEAM ELECTRIC STATION  
PROPOSED LICENSE AMENDMENT NO. 285  
FOR UNIT 1 OPERATING LICENSE NO. NPF-14  
AND PROPOSED LICENSE AMENDMENT NO. 253  
FOR UNIT 2 OPERATING LICENSE NO. NPF-22  
EXTENDED POWER UPRATE APPLICATION  
SUPPLEMENT TO REQUEST FOR ADDITIONAL  
INFORMATION RESPONSES  
PLA-6230**

---

**Docket Nos. 50-387  
and 50-388**

- References:*
- 1) *PPL Letter PLA-6076, B. T. McKinney (PPL) to USNRC, "Proposed License Amendment Numbers 285 For Unit 1 Operating License No. NPF-14 and 253 for Unit 2 Operating License No. NPF-22 Constant Pressure Power Uprate," dated October 11, 2006.*
  - 2) *PPL Letter PLA-6209, B. T. McKinney (PPL) to USNRC, "Proposed License Amendment Numbers 285 For Unit 1 Operating License No. NPF-14 and 253 for Unit 2 Operating License No. NPF-22 Reactor Systems Technical Review Request for Additional Information Responses," dated June 15, 2007.*
  - 3) *PPL Letter PLA-6155, B. T. McKinney (PPL) to USNRC, "Proposed License Amendment Numbers 285 For Unit 1 Operating License No. NPF-14 and 253 for Unit 2 Operating License No. NPF-22 Constant Pressure Power Uprate - Supplement," dated February 20, 2007.*
  - 4) *PPL Letter PLA-6175, B. T. McKinney (PPL) to USNRC, "Proposed License Amendment Numbers 285 For Unit 1 Operating License No. NPF-14 and 253 for Unit 2 Operating License No. NPF-22 Extended Application Regarding Steam Dryer and Flow Effects," dated April 17, 2007.*

Pursuant to 10 CFR 50.90, PPL Susquehanna LLC (PPL) requested in Reference 1 approval of amendments to the Susquehanna Steam Electric Station (SSES) Unit 1 and Unit 2 Operating Licenses (OLs) and Technical Specifications (TSs) to increase the maximum power level authorized from 3489 Megawatts Thermal (MWt) to 3952 MWt, an approximate 13% increase in thermal power. The proposed Constant Pressure Power Uprate (CPPU) represents an increase of approximately 20% above the Original Licensed Thermal Power (OLTP).

A001

NRR

Reference 2 identified that responses to NRC Questions 3, 4 and 8 will be provided by June 22, 2007. Attachment 1 and 4 herein provides the responses.

In addition, in a teleconference call between PPL and the NRC Staff held on June 6, 2007, the staff requested supplemental information be provided to assist with their review. The supplemental information requested during this teleconference is also provided in Attachment 1.

Attachments 1 and 4 contain AREVA NP, Inc. proprietary information. As such, AREVA NP, Inc. requests that they be withheld from public disclosure in accordance with 10 CFR 2.390 (a) 4 and 9.17 (a) 4. Affidavits supporting this request are contained in Attachment 4. Attachment 2 contains a non-proprietary version of Attachment 1.

There are no regulatory commitments associated with this submittal.

PPL has reviewed the "No Significant Hazards Consideration" and the "Environmental Consideration" submitted with Reference 1 relative to the Enclosure. We have determined that there are no changes required to either of these documents.

If you have any questions or require additional information, please contact Mr. Michael H. Crowthers at (610) 774-7766.

I declare under perjury that the foregoing is true and correct.

Executed on: 6-27-07



B. T. McKinney

Attachment 1: Proprietary Version of the Request for Additional Information Responses

Attachment 2: Non-Proprietary Version of the Request for Additional Information Responses

Attachment 3: (1) EMF-3153(P), (2) EMF-3154(P), (3) K. H. Sun and R. T. Fernandez, "Countercurrent Flow Limitation Correlation for BWR Bundles During LOCA" (4) OhKawa-Lahey, "The Analysis of Proposed BWR Inlet Flow Blockage Experiments in PBF"

Attachment 4: AREVA NP, Inc. Affidavits

Copy: NRC Region I

Mr. A. J. Blamey, NRC Sr. Resident Inspector

Mr. R. V. Guzman, NRC Sr. Project Manager

Mr. R. R. Janati, DEP/BRP

---

**Attachment 4 to PLA-6230  
AREVA NP, Inc. Affidavit**

---



withheld from public disclosure. The request for withholding of proprietary information is made in accordance with 10 CFR 2.390. The information for which withholding from disclosure is requested qualifies under 10 CFR 2.390(a)(4) "Trade secrets and commercial or financial information".

6. The following criteria are customarily applied by AREVA NP to determine whether information should be classified as proprietary:

- (a) The information reveals details of AREVA NP's research and development plans and programs or their results.
- (b) Use of the information by a competitor would permit the competitor to significantly reduce its expenditures, in time or resources, to design, produce, or market a similar product or service.
- (c) The information includes test data or analytical techniques concerning a process, methodology, or component, the application of which results in a competitive advantage for AREVA NP.
- (d) The information reveals certain distinguishing aspects of a process, methodology, or component, the exclusive use of which provides a competitive advantage for AREVA NP in product optimization or marketability.
- (e) The information is vital to a competitive advantage held by AREVA NP, would be helpful to competitors to AREVA NP, and would likely cause substantial harm to the competitive position of AREVA NP.

The information in the Document is considered proprietary for the reasons set forth in paragraphs 6(b) and 6(c) above.

7. In accordance with AREVA NP's policies governing the protection and control of information, proprietary information contained in this Document have been made available,

on a limited basis, to others outside AREVA NP only as required and under suitable agreement providing for nondisclosure and limited use of the information.

8. AREVA NP policy requires that proprietary information be kept in a secured file or area and distributed on a need-to-know basis.

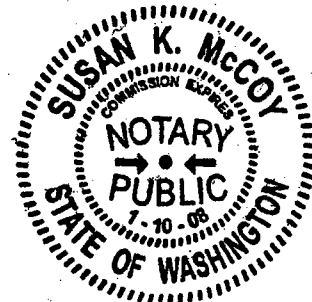
9. The foregoing statements are true and correct to the best of my knowledge, information, and belief.

Jerald S Holm

SUBSCRIBED before me this 14<sup>th</sup>  
day of June, 2007.

Susan K McCoy

Susan K. McCoy  
NOTARY PUBLIC, STATE OF WASHINGTON  
MY COMMISSION EXPIRES: 1/10/2008





requested qualifies under 10 CFR 2.390(a)(4) "Trade secrets and commercial or financial information".

6. The following criteria are customarily applied by AREVA NP to determine whether information should be classified as proprietary:

- (a) The information reveals details of AREVA NP's research and development plans and programs or their results.
- (b) Use of the information by a competitor would permit the competitor to significantly reduce its expenditures, in time or resources, to design, produce, or market a similar product or service.
- (c) The information includes test data or analytical techniques concerning a process, methodology, or component, the application of which results in a competitive advantage for AREVA NP.
- (d) The information reveals certain distinguishing aspects of a process, methodology, or component, the exclusive use of which provides a competitive advantage for AREVA NP in product optimization or marketability.
- (e) The information is vital to a competitive advantage held by AREVA NP, would be helpful to competitors to AREVA NP, and would likely cause substantial harm to the competitive position of AREVA NP.

The information in the Document is considered proprietary for the reasons set forth in paragraphs 6(b) and 6(c) above.

7. In accordance with AREVA NP's policies governing the protection and control of information, proprietary information contained in this Document have been made available, on a limited basis, to others outside AREVA NP only as required and under suitable agreement providing for nondisclosure and limited use of the information.

8. AREVA NP policy requires that proprietary information be kept in a secured file or area and distributed on a need-to-know basis.

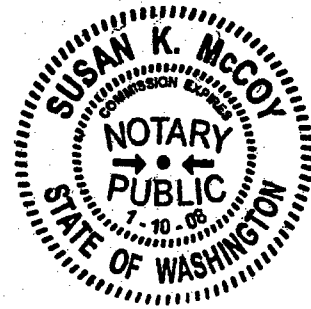
9. The foregoing statements are true and correct to the best of my knowledge, information, and belief.

Jerald S Holm

SUBSCRIBED before me this 14th  
day of June, 2007.

Susan K McCoy

Susan K. McCoy  
NOTARY PUBLIC, STATE OF WASHINGTON  
MY COMMISSION EXPIRES: 1/10/2008





requested qualifies under 10 CFR 2.390(a)(4) "Trade secrets and commercial or financial information".

6. The following criteria are customarily applied by AREVA NP to determine whether information should be classified as proprietary:

- (a) The information reveals details of AREVA NP's research and development plans and programs or their results.
- (b) Use of the information by a competitor would permit the competitor to significantly reduce its expenditures, in time or resources, to design, produce, or market a similar product or service.
- (c) The information includes test data or analytical techniques concerning a process, methodology, or component, the application of which results in a competitive advantage for AREVA NP.
- (d) The information reveals certain distinguishing aspects of a process, methodology, or component, the exclusive use of which provides a competitive advantage for AREVA NP in product optimization or marketability.
- (e) The information is vital to a competitive advantage held by AREVA NP, would be helpful to competitors to AREVA NP, and would likely cause substantial harm to the competitive position of AREVA NP.

The information in the Document is considered proprietary for the reasons set forth in paragraphs 6(b) and 6(c) above.

7. In accordance with AREVA NP's policies governing the protection and control of information, proprietary information contained in this Document have been made available, on a limited basis, to others outside AREVA NP only as required and under suitable agreement providing for nondisclosure and limited use of the information.

8. AREVA NP policy requires that proprietary information be kept in a secured file or area and distributed on a need-to-know basis.

9. The foregoing statements are true and correct to the best of my knowledge, information, and belief.

Jerald Holan

SUBSCRIBED before me this 14<sup>th</sup>  
day of June, 2007.

Susan K. McCoy

Susan K. McCoy  
NOTARY PUBLIC, STATE OF WASHINGTON  
MY COMMISSION EXPIRES: 1/10/2008



---

**Attachment 2 to PLA-6230**  
**Non-Proprietary Version of the Request for**  
**Additional Information Responses**

---

**The following provides the responses to NRC Questions 3, 4 and 8 contained in the Request for Additional Information Responses transmitted to NRC in References 2. The NRC Question and PPL Response for each is provided below.**

**Note, in the PPL Responses that follow, the references are listed at the end of each response.**

**NRC Question 3:**

(Fuel System Design): The staff is unable to determine from Technical Specification (TS) 5.6.5.b, "Core Operating Limits Report," and PUSAR Table 1-1, as to which methods specified perform which function. The staff is also unable to determine whether each specified method is being used in a manner consistent with its NRC approval. Supplement both the Core Operating Limits Report (COLR) references list and Table 1-1 with a specific description of the function of each method and explaining why, in some cases, as many as six codes are required to perform a task or group of tasks.

**PPL Response:**

Table 1-1 of the PUSAR identifies tasks and the related computer codes used in analyses performed to support the Susquehanna CPPU project. The COLR reference list (SSES Unit 1 and 2 Technical Specification Section 5.6.5) contains those NRC approved methods used to determine the core operating limits. The References common to PUSAR Table 1-1 and the current SSES TS's that were used to support the CPPU analyses are COLR references 1, 5-7, 9-11 and 14. Current SSES TS COLR references 16 and 17 are being deleted as part of the CPPU. The rest of the COLR references are not needed for CPPU analyses. The tasks identified in PUSAR Table 1-1 that involve ATRIUM<sup>TM</sup>10<sup>4</sup> fuel and AREVA NP<sup>5</sup> methods are:

- (a) Reactor core and fuel performance
- (b) Safety limit MCPR
- (c) Transient analysis
- (d) LOCA-ECCS
- (e) Appendix R – fire protection
- (f) Reactor core stability

For each PUSAR Table 1-1 task identified above, the analyses performed for the task, the codes used for each analysis, the function of each code in the analysis, and how the use of the code is consistent with NRC approval are described below.

---

<sup>1</sup> ATRIUM is a trademark of AREVA NP.

<sup>2</sup> AREVA NP Inc. is an AREVA and Siemens company.

(a) **Reactor Core and Fuel Performance**

The reactor core and fuel performance are modeled with the CASMO-4/MICROBURN-B2 (Reference A.1) code system. This neutronics code system is utilized in the core design process to determine the core loading pattern, develop control rod patterns for the cycle step-through, evaluate cold shutdown margin, and determine margin to thermal limits. In addition, the CASMO-4/MICROBURN-B2 code system is used to evaluate quasi-steady-state licensing analyses, provide input to other safety analyses, and perform core monitoring functions.

The CASMO-4 code is the lattice spectrum/depletion code and is a multi-group, 2-dimensional transport theory code. CASMO-4 homogenizes the heterogeneous lattice spectrum into a neutronicly equivalent homogeneous medium, determines pin power distributions, and depletes nuclides in fuel and burnable absorber pins. The output data from CASMO-4 is processed into a lattice neutronic data library for the MICROBURN-B2 core simulator code.

The MICROBURN-B2 code determines core wide nodal exposure and nuclide density distributions, channel inlet flow distribution, and fuel thermal performance parameters such as minimum critical power ratio (MCPR), linear heat generation rate (LHGR), and maximum average planar linear heat generation rate (MAPLHGR).

Figure A.1 shows the computer codes and calculational process used in the neutronics modeling of the fuel and reactor core. CAZAM, ALAADIN, AUTOXSEC, CDM, AUTOCDR, MB2STF, PRECOT2, and AUTOCOT are automation codes used to either prepare inputs or process data transferred between codes. All automation codes are fully qualified and are documented according to AREVA prescribed procedures.

The acceptability of the CASMO-4/MICROBURN-B2 methodology for BWR licensing analyses and core monitoring applications is documented in Reference A.1 and in the SER prepared by the NRC. The SER restrictions associated with Reference A.1 are:

1. The CASMO-4/MICROBURN-B2 code system shall be applied in a manner that predicted results are within the range of the validation criteria (Tables 2.1 and 2.2) and measurement uncertainties (Table 2.3) presented in EMF-2158(P).

2. The CASMO-4/MICROBURN-B2 code system shall be validated for analyses of any new fuel design which departs from current orthogonal lattice designs and/or exceed gadolinia and U-235 enrichment limits.
3. The CASMO-4/MICROBURN-B2 code system shall only be used for BWR licensing analyses and BWR core monitoring applications.
4. The review of the CASMO-4/MICROBURN-B2 code system should not be construed as a generic review of the CASMO-4 or MICROBURN-B2 computer codes.
5. The CASMO-4/MICROBURN-B2 code system is approved as a replacement for the CASMO-3/MICROBURN-B code system used in NRC-approved AREVA BWR licensing methodology and in AREVA BWR core monitoring applications. Such replacements shall be evaluated to ensure that each affected methodology continues to comply with its SER restrictions and/or conditions.
6. AREVA shall notify any customer who proposes to use the CASMO-4/MICROBURN-B2 code system independent of any AREVA fuel contract that conditions 1–4 above must be met. AREVA's notification shall provide positive evidence to the NRC that each customer has been informed by AREVA of the applicable conditions for using the code system.

Conformance to restriction 1 is addressed through benchmarking of the core system against previous cycles. The SSES CPPU design and analyses do not depart from the lattice designs nor do they exceed the U-235 enrichment and gadolinia limits approved in Reference A.1; thus restriction 2 is in conformance. The CASMO-4 /MICROBURN-B2 code system is only used for BWR applications and is therefore consistent with restriction 3. Conformance to restrictions 4 and 5 are implemented in AREVA engineering guidelines. AREVA conforms to restriction 6 by providing a copy of Reference A.1, which includes the SER to customers who use CASMO-4/MICROBURN-B2.

In addition to performing reload core design analyses, the CASMO-4/MICROBURN-B2 code system is also used to perform certain steady-state or quasi-steady-state safety analyses and to provide neutronic input to other safety analyses codes.

The following AOO, accident, and other neutronic analyses are performed with the CASMO-4/MICROBURN-B2 code system:

- Cold shutdown margin
- Standby boron liquid control
- Control rod withdrawal error
- Loss of feedwater heating
- Control rod drop accident
- Fuel loading error (includes mislocation and misorientation)
- Core flow increase event Linear Heat Generation Rate (LHGR<sub>f</sub>)

Cold shutdown margin (CSDM) is the evaluation of core reactivity at cold conditions with strongest control rod withdrawn, all other rods fully inserted. (CSDM is evaluated on a cycle-specific basis.)

Standby liquid control (SLC) is reactivity control by injection of boron in moderator (typically 660 ppm B). The SLC system must be able to render the core subcritical in the event control rods become inoperable. (This event is assessed on a cycle-specific basis.)

The control rod withdrawal error (CRWE) event is the inadvertent withdrawal of a control rod at power until it is stopped by the rod block monitor (RBM) on BWR 4 plants such as SSES. (This event is analyzed on a cycle-specific basis for BWR 4 plants.)

The loss of feedwater heating (LFWH) event is the loss of feedwater heating capability due to the closing of a steam extraction line or the bypassing of feedwater flow around a heater, causing insertion of reduced temperature water into the core at power, i.e., reactivity insertion ( $\Delta\text{CPR}$ ). (Reference A.15 is the generic topical report which uses MICROBURN-B2 methodology.)

The control rod drop accident (CRDA) analysis assumes that during startup a control rod becomes decoupled from its drive, sticks, then falls to the new drive position during control rod withdrawals. High rod worths are avoided primarily by implementation of BPWS (banked position withdrawal sequence). Rods calculated to have deposited enthalpies  $>170$  cal/g are assumed to fail and are compared to the offsite dose criteria. (This event is assessed on a cycle-specific basis.)

The fuel loading error is the inadvertent misplacement of a fuel bundle in either a wrong core location or misrotated in a cell. Bounding analyses have been performed for both the fuel loading and misorientation events. The continued applicability of these bounding analyses is confirmed on a cycle-specific basis.

For the core flow increase event, the recirculation pumps are assumed to be operating at a reduced flow condition and then “runout” to their maximum speed increasing the core recirculation flow rate. On a cycle-specific basis, CASMO-4/MICROBURN-B2 calculates the initial and final conditions of this slow transient event. This calculation identifies conditions where the LHGR limit should be decreased for low flow conditions ( $LHGR_f$ ) and also provides input for the flow dependent MCPR calculation, ( $MCPR_f$ ).

The CASMO-4/MICROBURN-B2 code system is used for neutronic input for Safety Limit MCPR, Operating Limit MCPR, transient analyses, LOCA, and stability analyses which are all discussed in detail below.

**(b) Safety Limit and Operating Limit MCPR**

The operation of a BWR requires protection against fuel damage during normal reactor operation and AOOs. A rapid decrease in heat removal capacity associated with boiling transition could result in high temperatures in the cladding, which may cause cladding degradation and a loss of fuel rod integrity. Protection of the fuel against boiling transition ensures that such degradation is avoided. This protection is accomplished by determining the operating limit minimum critical power ratio (Operating Limit MCPR) each cycle.

The AREVA thermal limits analysis methodology, THERMEX, is described in Reference A.3. The thermal limits methodology in THERMEX consists of a series of related analyses which establish an Operating Limit MCPR (OLMCPR). The OLMCPR is determined from two calculated values, the Safety Limit MCPR (SLMCPR) and the limiting transient analysis  $\Delta$ CPR (Figure 3.2).

Reference A.4 provides the basis for the AREVA methodology for determining the SLMCPR that ensures that 99.9% of the fuel rods are expected to avoid boiling transition. The SLMCPR is determined by statistically combining calculation uncertainties and plant measurement uncertainties that are associated with the calculation of MCPR. This determination is carried out by a series of Monte Carlo calculations in which the variables affecting boiling transition are randomly varied and the total number of rods experiencing boiling transition is determined for each Monte Carlo trial. The expected number of rods in boiling transition is determined from the probability distribution created from the Monte Carlo trials and a

[ ] If the expected values of rods in boiling transition is less than 0.1%, the selected SLMCPR is supported (Figure 3.3).

Figure 3.4 shows the computer codes and calculation process used in the SLMCPR analysis.

The SAFLIM2 computer code is used to calculate the number of fuel rods in the core expected to experience boiling transition for a specified core MCPR. SAFLIM2 implements the methodology described in Reference A.4. SAFLIM2 is used to determine the SLMCPR.

The fuel assembly flow characteristics used in the SAFLIM2 code are obtained from the XCOBRA computer code. XCOBRA is used to evaluate core thermal-hydraulic performance and calculate fuel assembly hydraulic demand curves (HDC). The HDC generated using XCOBRA are input to SAFLIM2. As described in Reference A.3, the XCOBRA code is a steady-state version of the thermal-hydraulic code XCOBRA-T (Reference A.6).

The power distributions used in the SLMCPR analysis are obtained from the MICROBURN-B2 and CASMO-4 computer codes discussed in Section (a). The assembly radial peaking factors (RPFs) and core axial power shape are obtained from MICROBURN-B2. The fuel rod local peaking factors (LPFs) for each fuel assembly are obtained from CASMO-4.

The SLPREP computer code shown in Figure 3.4 is an automation code used to collect data and prepare input for the SAFLIM2 code.

The acceptability of the THERMEX methodology and the XCOBRA code for licensing analyses is documented in Reference A.3 and in the SER prepared by the NRC. The SER restriction associated with Reference A.3 is:

1. Monitoring systems other than POWERPLEX<sup>®</sup> may be used provided that the associated power distribution uncertainties are identified and appropriate operating parameters compatible with transient safety analyses are monitored. Whatever monitoring system is used should be specifically identified in plant submittals.

The SER restriction is implemented in AREVA engineering guidelines. SSES uses POWERPLEX.

The acceptability of the SLMCPR methodology for licensing analyses is documented in Reference A.4 and in the SER prepared by the NRC. The SER restrictions associated with Reference A.4 are:

1. The NRC approved MICROBURN-B power distribution uncertainties should be used in the SLMCPR determination.
2. Since the ANFB correlation uncertainties depend on fuel design, in plant-specific applications the uncertainty value used for the ANFB additive constants should be verified.
3. The CPR channel bowing penalty for non-ANF fuel should be made using conservative estimates of the sensitivity of local power peaking to channel bow.
4. The methodology for evaluating the effect of fuel channel bowing is not applicable to reused second-lifetime fuel channels.

SER restrictions 1 and 2 are implemented in AREVA engineering guidelines and automation tools. Note: MICROBURN-B was subsequently replaced by MICROBURN-B2 and ANFB was subsequently replaced by SPCB. Restrictions 3 and 4 are implemented in AREVA engineering guidelines.

(c) **Transient Analysis**

Transient analyses are performed to demonstrate that the fuel performs within design criteria during anticipated operational occurrences (AOOs) and to establish operating limits for the reactor. To protect the established SLMCPR, evaluations of AOOs are performed which produce the limiting transient  $\Delta$ CPR, that when added to the SLMCPR, defines the OLMCPR. Potentially limiting AOOs, including generator load rejection without bypass and feedwater controller failure, are evaluated using the transient analysis methodology. The methodology used for the analysis of these events is found in References A.1, A.3, A.5, A.6, and A.7.

Figure 3.5 shows the computer codes and calculation process used in the evaluation of transient analyses.

RODEX2 predicts the thermal and mechanical performance of BWR fuel rods as a function of power history. RODEX2 is used to provide initial conditions for transient and accident analyses (hot channel and core average fuel rod gap conductance).

MICROBURN-B2 is used in conjunction with PRECOT2 to build the core cross-section deck (COTRAN deck) for the state point of interest (power, flow, exposure).

COTRANSA2 is a BWR system transient analysis code with models representing the reactor core, reactor vessel, steam lines, recirculation loops, and control systems. COTRANSA2 is used to evaluate key reactor system parameters such as power, flow, pressure, and quality during core-wide BWR transient events and provide boundary conditions for hot channel analyses performed to calculate  $\Delta$ CPR.

XCOBRA predicts the steady-state thermal-hydraulic performance of BWR cores at various operating conditions and power distributions. XCOBRA is used to generate hot channel flow rates as a function of hot channel radial peaking factors. XCOBRA-T predicts the transient thermal-hydraulic performance of BWR cores during postulated system transients. XCOBRA-T is used to evaluate the transient thermal-hydraulic response of individual fuel assemblies in the core during transient events and to evaluate the  $\Delta$ CPR for the limiting fuel assemblies in the core during system transients. [

]

The acceptability of the RODEX2 code for licensing analyses is documented in Reference A.7 and in the SER prepared by the NRC. The SER restrictions associated with Reference A.7 are:

1. The NRC concluded that the RODEX2 fission gas release model was acceptable to burnups up to 60 MWd/KgU. This implies a burnup limit of 60 MWd/KgU (nodal basis).
2. The creep correlation accepted by the NRC is the one with the designation MTYPE=0.

SER restriction 1 no longer applies. The exposure limits for BWR fuel were increased to 54 MWd/kgU for an assembly and to 62 MWd/kgU for a rod in Reference A.9. Restriction 2 is implemented in AREVA engineering guidelines and through computer code controls (defaults, override warning messages). The acceptability of the MICROBURN-B2 and CASMO-4 codes for licensing analyses is documented in Reference A.1 and discussed in Section (a).

The acceptability of the COTRANSA2 code for licensing analyses is documented in Reference A.5 and in the SER prepared by the NRC. The SER restrictions associated with Reference A.5 are:

1. Use of COTRANSA2 is subject to limitations set forth for methodologies described and approved for XCOBRA-T and COTRAN.
2. The COTRANSA2 code is not applicable to the analysis of any transient for which lateral flow in a bundle is significant and nonconservative in the calculation of system response.
3. For those analyses in which core bypass is modeled, the effect of a computed negative flow in the core bypass region should be shown to make no significant nonconservative contribution in the system response.
4. Licensing applications referencing the COTRANSA2 methodology must include confirmation that sensitivity to the time step selection has been considered in the analysis.

SER restrictions 1, 2, and 4 are implemented in AREVA engineering guidelines. Restriction 3 is implemented in AREVA engineering guidelines and automation tools.

The acceptability of the XCOBRA code for licensing analyses is documented in Reference A.3 and discussed in Section (b).

The acceptability of the XCOBRA-T code for licensing analyses is documented in Reference A.6 and in the SER prepared by the NRC. The SER restrictions associated with Reference A.6 are:

1. XCOBRA-T was found acceptable (References A.14 and A.16) for the analysis of only the following licensing basis transients:
  - a. Load rejection without bypass
  - b. Turbine trip without bypass
  - c. Feedwater controller failure
  - d. Steam isolation valve closure without direct scram
  - e. Loss of feedwater heating or inadvertent high pressure coolant injection (HPCI) actuation
  - f. Flow increase transients from low-power and low-flow operation

2. XCOBRA-T analyses that result in any calculated downflow in the bypass region will not be considered valid for licensing purposes.
3. XCOBRA-T licensing calculations must use NRC approved default options for void-quality relationship and two-phase multiplier correlations.
4. The use of XCOBRA-T is conditional upon a commitment by ENC to a follow-up program to examine the XCOBRA-T void profile against experimental data from other sources.

SER restrictions 1, 2, and 3 are implemented in AREVA engineering guidelines. SER restriction 3 is also implemented through code controls (defaults, override warning messages). Restriction 4 was subsequently addressed in Reference A.8 and no further action is required.

**(d) LOCA-ECCS**

Plant specific LOCA-ECCS analyses are performed to demonstrate that fuel MAPLHGR limits are adequate to ensure that 10 CFR 50.46 acceptance criteria are met during a postulated LOCA. LOCA break spectrum analyses are performed to determine the characteristics of the limiting LOCA event. The characteristics evaluated in the break spectrum analysis include ECCS single failure, break location, break size, and axial power shape. For the limiting LOCA event, fuel assembly heatup calculations are performed to determine the peak cladding temperature (PCT) and metal-water reaction (MWR) values over the exposure lifetime of the fuel when operating at the MAPLHGR limit. Figure 3.6 shows the computer codes and calculation process used in LOCA-ECCS analyses.

RODEX2 is a fuel rod performance code used to predict the thermal-mechanical behavior of BWR fuel rods as a function of exposure and power history. Fuel rod characteristics (such as stored energy) prior to the LOCA are calculated using RODEX2 and are used as input for other LOCA analysis codes.

RELAX is a BWR systems analysis code with models representing the reactor core, reactor vessel, recirculation lines, and ECCS systems. RELAX is used to calculate both the reactor system and the core hot channel response during a LOCA. The RELAX system analysis is used to calculate the reactor system fluid conditions used as boundary conditions for the hot channel analysis. The RELAX

hot channel calculation provides fluid conditions and heat transfer coefficients for the heatup calculation during the blowdown phase of the LOCA. Appendix K spray heat transfer coefficients are used in the heatup calculation after the end of blowdown.

HUXY is a heat transfer code used to calculate the heatup of the peak power plane in a BWR fuel assembly during the blowdown, refill, and reflood phases of a LOCA. HUXY is used to calculate PCT and MWR for the fuel assembly during a LOCA.

The acceptability of the RODEX2 code for licensing analyses is documented in Reference A.7 and in the SER prepared by the NRC. The SER restrictions associated with Reference A.7 are discussed in Section I.

The acceptability of the RELAX code for licensing analyses is documented in Reference A.10 and in the SER prepared by the NRC. The SER restriction associated with Reference A.10 is:

- (a) The staff concluded that the EXEM BWR-2000 Evaluation Model was acceptable for referencing in BWR LOCA analysis, with the limitation that the application of the revised evaluation model be limited to jet pump applications.

The SER restriction is implemented in AREVA engineering guidelines. SSES has jet pumps.

The acceptability of the HUXY code for licensing analyses is documented in Reference A.11 and in the SER prepared by the NRC. The SER restrictions associated with Reference A.11 are:

1. The staff, however, will require that a conservative reduction of 10% be made in the (spray heat transfer) coefficients specified in 10 CFR 50 Appendix K for 7x7 assemblies when applied to ENC 8x8 assemblies.
2. In each individual plant submittal employing the Exxon model, the applicant will be required to properly take rod bowing in account.
3. Since GAPEX is not identical to HUXY in radial nodding or solution scheme, it is required that the volumetric average fuel temperature for each rod be equal to or greater than that in the approved version of GAPEX. If it is not, the gap coefficient must be adjusted accordingly.

4. It has been demonstrated that the (2DQ local quench velocity) correlation gives hot plane quench time results that are suitably conservative with respect to the available data when a coefficient behind the quench front of 14,000 Btu/(hr-ft<sup>2</sup>-°F) is used.
5. It (Appendix K) requires that heat production from the decay of fission products shall be 1.2 times the value given by K. Shure as presented in ANS 5.1 and shall assume infinite operation time for the reactor.
6. It is to be assumed for all these heat sources (fission heat, decay of actinides and fission product decay) that the reactor has operated continuously at 102% of licensed power at maximum peaking factors allowed by Technical Specifications.
7. For small and intermediate size breaks, the applicability of the fission power curve used in the calculations will be justified on a case-by-case basis. This will include justification of the time of scram (beginning point in time of the fission power decrease) and the rate of fission power decrease due to voiding, if any.
8. The rate of (metal water) reaction must be calculated using the Baker-Just equation with no decrease in reaction rate due to the lack of steam. This rate equation must be used to calculate metal-water reactions both on the outside surface of the cladding, and if ruptured, on the inside surface of the cladding. The reaction zone must extend axially at least 3 inches.
9. The initial oxide thickness (that affects the zirconium-water reaction rate) used should be no larger than can be reasonably justified, including consideration of the effects of manufacturing processes, hot-functional testing and exposure.
10. Exxon has agreed to provide calculations on a plant by plant basis to demonstrate that the plane of interest assumed for each plant is the plane in which peak cladding temperatures occur for that plant.

SER restrictions 1, 2, 3, 4, 6, 7, 9, and 10 are implemented in AREVA engineering guidelines. Restrictions 5 and 8 are directly implemented in engineering computer codes.

The use of Appendix K spray heat transfer coefficients for the ATRIUM-10 fuel design is justified in Reference A.12. There are no SER restrictions associated with Reference A.12.

(e) **Appendix R – Fire Protection**

Analyses are performed to ensure compliance with the requirements of 10 CFR 50 Appendix R relative to fire protection. These analyses involve assessing the ability to shutdown the reactor after a loss of off-site power and the loss of specified plant equipment due to a fire at the plant. [

]

(f) **Reactor Core Stability**

In order to ensure compliance with the licensing criteria set forth in 10 CFR 50 GDC 12, the Long Term Stability Solution Option III setpoints need to be appropriately set. The Detect and Suppress (D&S) Option III solution depends on timely detection of oscillatory behavior by applying certain algorithms to the signals of several OPRMs. The methodology used to demonstrate that the timely suppression of the growing oscillation by reactor scram ensures that the SLMCPR is not violated consists of the following components:

1. Determination of the minimum critical power ratio (MCPR) margin that exists prior to the onset of the oscillation. This is a plant- and cycle-specific calculation that determines the minimum expected MCPR based on two specified scenarios: a two recirculation pump trip from full power at the highest rod line and steady-state operation at 45% core flow at the operating limit MCPR.
2. The hot channel oscillation magnitude (HCOM) versus OPRM setpoint. This portion of the methodology is plant-specific and cycle independent and is typically calculated generically by the OPRM vendor.
3. The DIVOM curve. This is a conservative relationship between the change in CPR and the hot channel power oscillation magnitude.

The selection of an OPRM setpoint determines the maximum hot channel oscillation magnitude based on the HCOM curve. The corresponding change in CPR due to the oscillation is determined using the DIVOM curve. Next, the change in CPR due to the oscillation is used to assess the margin to the SLMCPR given the initial MCPR. The optimum setpoint should be high enough to allow sufficient time for reliable oscillation detection, but must be low enough to preclude the violation of the MCPR safety limit. The determination of the setpoint is cycle-specific.

Figure 3.7 shows the computer codes and calculation process used in the OPRM setpoint analysis.

Reference A.13 provides the basis for the DIVOM methodology used in determining the OPRM setpoints. The RAMONA5-FA computer code is used to calculate the transient response of the core during out-of-phase core power oscillations. The RAMONA5-FA code implements the BWROG DIVOM methodology guidelines (i.e. Reference A.13) and has been audited by the NRC.

The cross sections, power distributions, and core loading used by RAMONA5-FA are obtained from the MICROBURN-B2 and CASMO-4 computer codes discussed in Section (a). This information is also used by the STAIF code. The STAIF code is used to determine the limiting channel decay ratio exposure which is used for sensitivity studies in RAMONA5-FA. In addition, MICROBURN-B2 is used to calculate the initial MCPR values at the state points of interest.

The DIVOMPLT computer code shown in Figure 3.7 is a post-processor used to calculate the DIVOM relationship from the transient power and CPR versus time information from RAMONA5-FA.

The acceptability of the STAIF code for licensing analyses is documented in Reference A.2 and in the SER prepared by the NRC. The SER restrictions associated with Reference A.2 are:

1. The SER concludes that the STAIF code is acceptable for best-estimate decay ratio calculations. This conclusion applies to the three types of instabilities relevant to BWR operation, which are quantified by the hot-channel, core-wide, and out-of-phase decay ratios. The staff estimates that STAIF decay ratio calculations for the decay ratio range of 0.0 to 1.1 are accurate within:

+/- 0.2 for the hot-channel decay ratio

+/- 0.15 for the core-wide decay ratio

+/- 0.2 for the out-of-phase decay ratio

2. The staff concludes that the proposed modification of the E1A acceptance criteria for region-validation calculations is acceptable because it provides the intended protection against instabilities outside the E1A regions. The following E1A region-validation criteria are acceptable for the STAIF code:

The calculated hot-channel decay ratio must be lower than 0.8.

The calculated core-wide decay ratio must be lower than 0.85.

The calculated out-of-phase decay ratio must be less than 0.8.

The SER restrictions are implemented in the AREVA engineering guidelines.

**References:**

- A.1 EMF-2158(P)(A) Revision 0, *Siemens Power Corporation Methodology for Boiling Water Reactors: Evaluation and Validation of CASMO-4/MICROBURN-B2*, Siemens Power Corporation, October 1999.
- A.2 EMF-CC-074(P)(A) Volume 4 Revision 0, *BWR Stability Analysis – Assessment of STAIF with Input from MICROBURN-B2*, Siemens Power Corporation, August 2000.
- A.3 XN-NF-80-19(P)(A) Volume 3 Revision 2, *Exxon Nuclear Methodology for Boiling Water Reactors, THERMEX: Thermal Limits Methodology Summary Description*, Exxon Nuclear Company, January 1987.
- A.4 ANF-524(P)(A) Revision 2 and Supplements 1 and 2, *ANF Critical Power Methodology for Boiling Water Reactors*, Advanced Nuclear Fuels Corporation, November 1990.
- A.5 ANF-913(P)(A) Volume 1 Revision 1 and Volume 1 Supplements 2, 3 and 4, *COTRANSA2: A Computer Program for Boiling Water Reactor Transient Analyses*, Advanced Nuclear Fuels Corporation, August 1990.
- A.6 XN-NF-84-105(P)(A) Volume 1 and Volume 1 Supplements 1 and 2, *XCOBRA-T: A Computer Code for BWR Transient Thermal-Hydraulic Core Analysis*, Exxon Nuclear Company, February 1987.
- A.7 XN-NF-81-58(P)(A) Revision 2 and Supplements 1 and 2, *RODEX2 Fuel Rod Thermal-Mechanical Response Evaluation Model*, Exxon Nuclear Company, March 1984.
- A.8 XN-NF-84-105(P)(A) Volume 1 Supplement 4, *XCOBRA-T: A Computer Code for BWR Transient Thermal-Hydraulic Core Analysis – Void Fraction Model Comparison to Experimental Data*, Advanced Nuclear Fuels Corporation, June 1988.
- A.9 EMF-85-74(P) Revision 0 Supplement 1(P)(A) and Supplement 2(P)(A), *RODEX2A (BWR) Fuel Rod Thermal-Mechanical Evaluation Model*, Siemens Power Corporation, February 1998.
- A.10 EMF-2361(P)(A) Revision 0, *EXEM BWR-2000 ECCS Evaluation Model*, Framatome ANP, May 2001.

- A.11 XN-CC-33(A) Revision 1, *HUXY: A Generalized Multirod Heatup Code with 10 CFR 50 Appendix K Heatup Option Users Manual*, Exxon Nuclear Company, November 1975.
- A.12 EMF-2292(P)(A) Revision 0, *ATRIUM™-10 Appendix K Spray Heat Transfer Coefficients*, Siemens Power Corporation, September 2000.
- A.13 BAW-10255(P) Revision 2, *Cycle-Specific DIVOM Methodology Using the RAMONA5-FA Code*, Framatome ANP, January 2006.
- A.14 Letter, Stuart Richards (NRC) to James F. Mallay (SPC), "Siemens Power Corporation Re: Request for Concurrence on Safety Evaluation Report Clarifications (TAC No. MA6160)," May 31, 2000.
- A.15 ANF-1358(P)(A) Revision 3, *The Loss of Feedwater Heating Transient in Boiling Water Reactors*, Framatome ANP, September 2005.

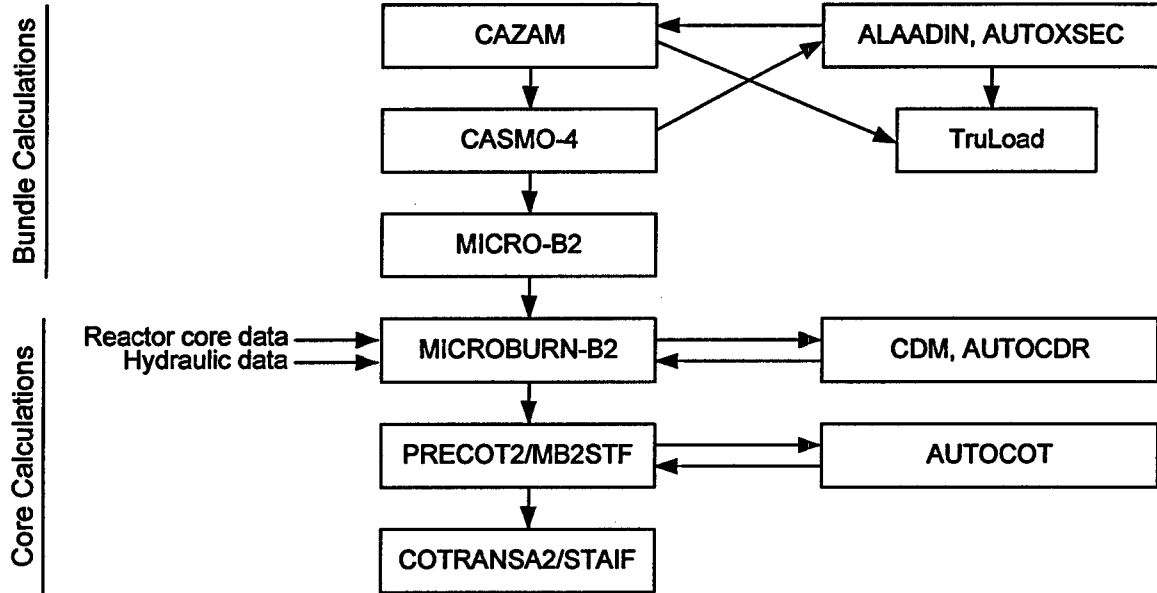


Figure 3.1 Neutronic Code Input Flow

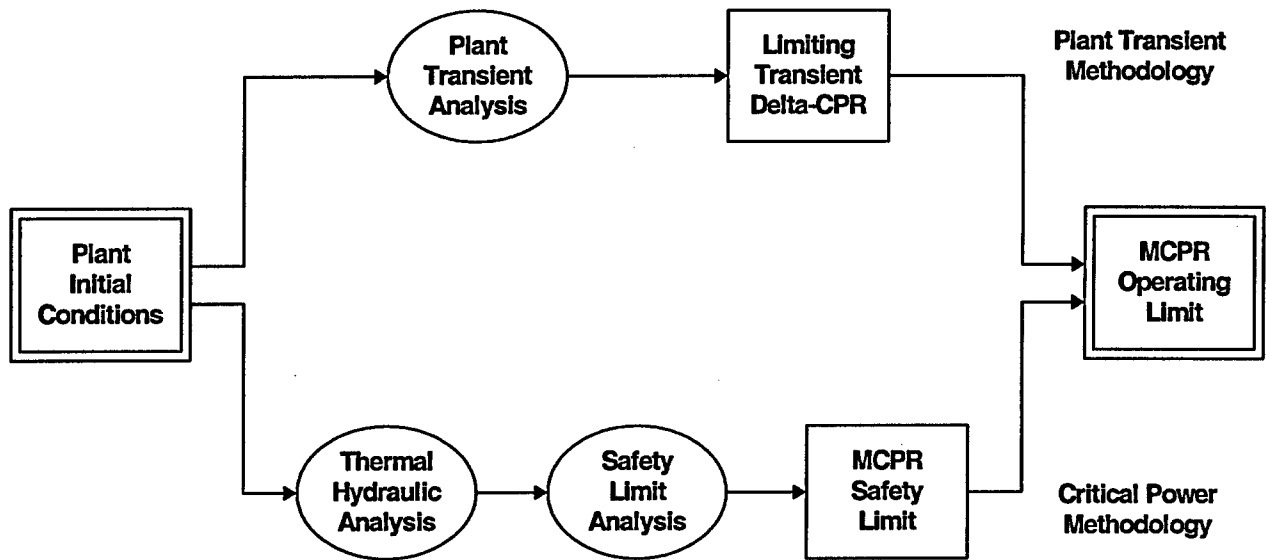
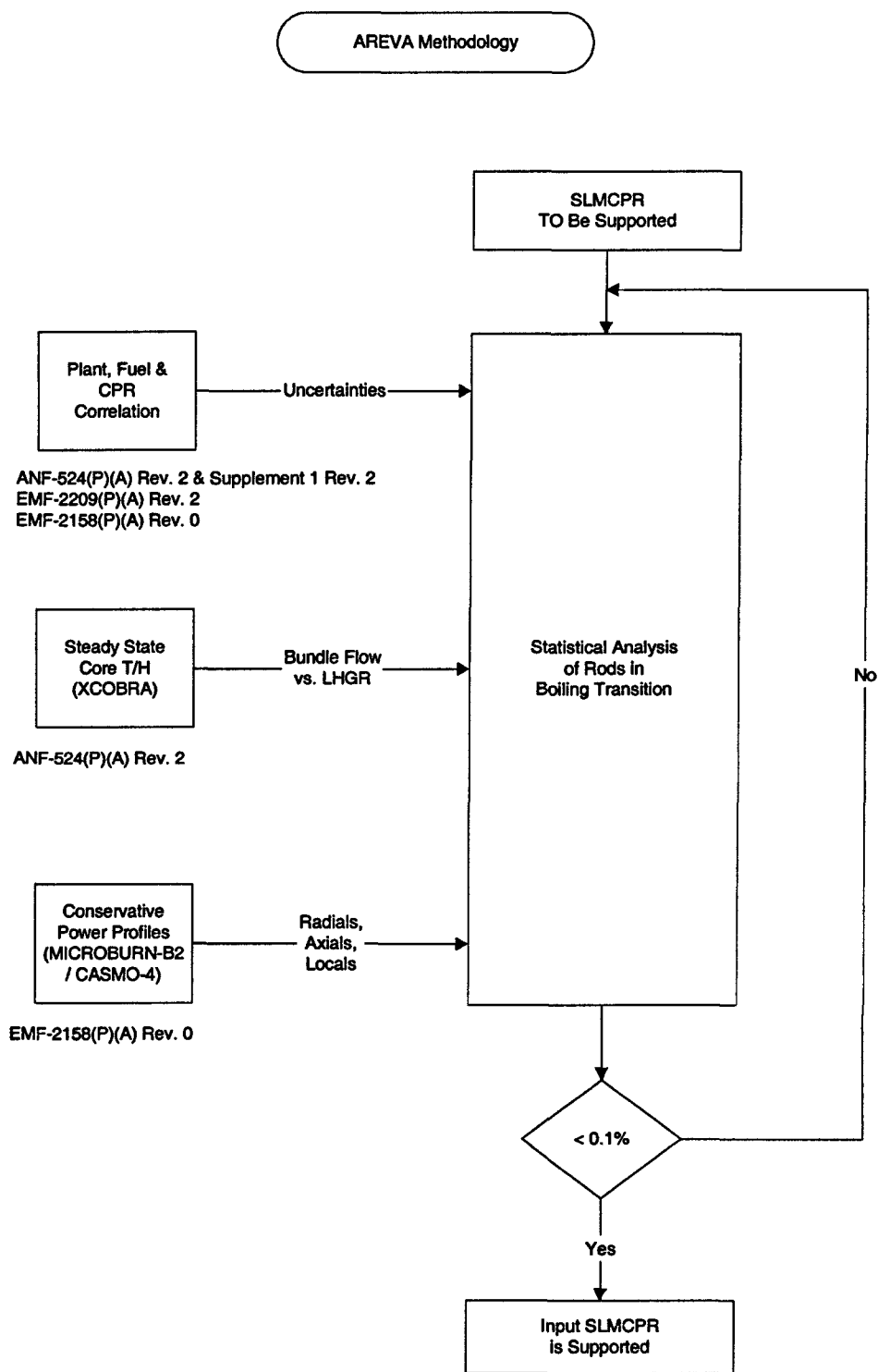
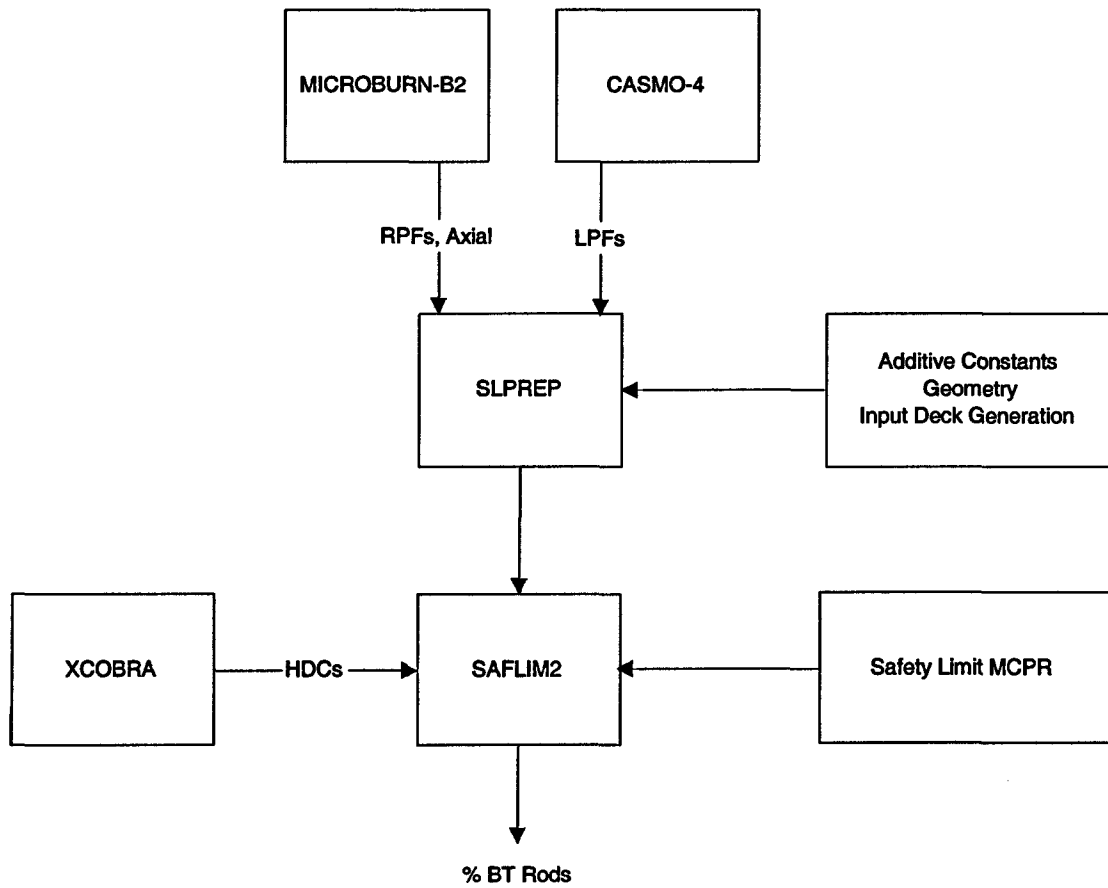


Figure 3.2 THERMEX Methodology



**Figure 3.3 SLMCPR Methodology**



**Figure 3.4 SLMCPR Calculation Process**

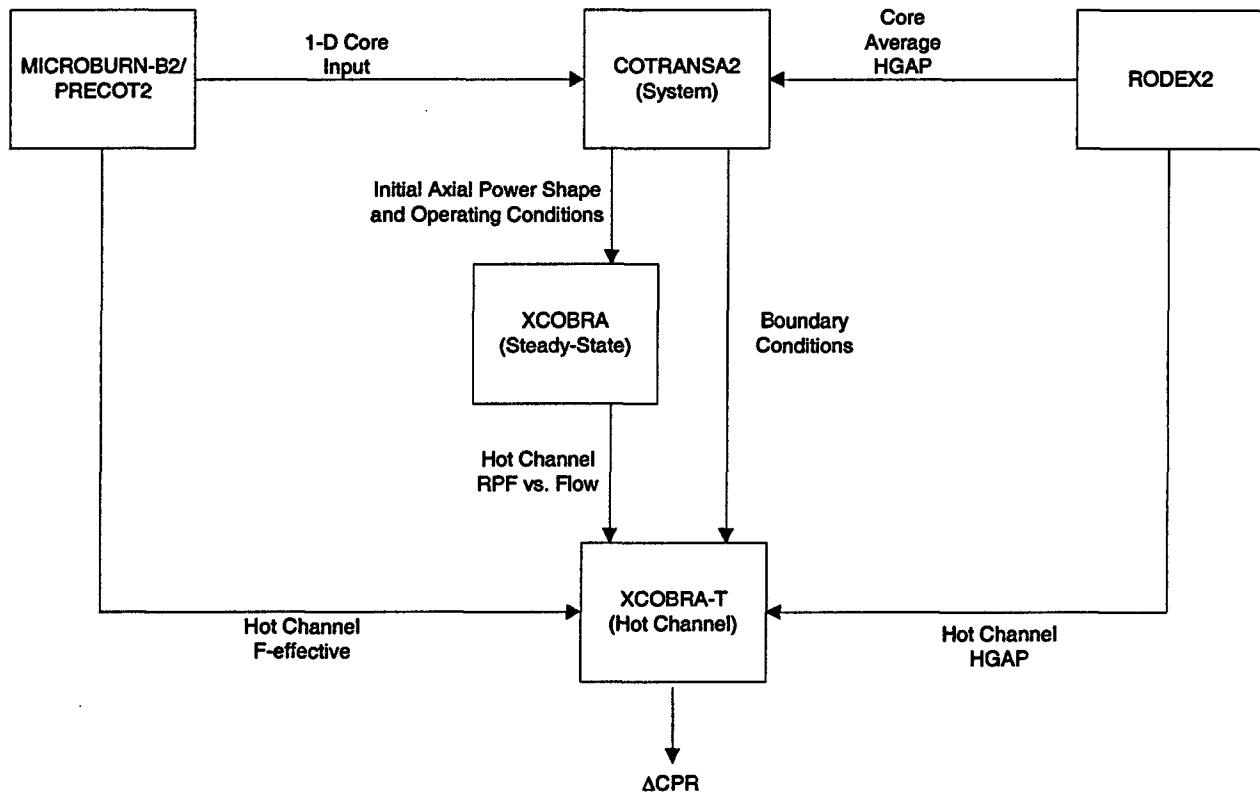


**Figure 3.5 Transient Analysis Calculation Process**

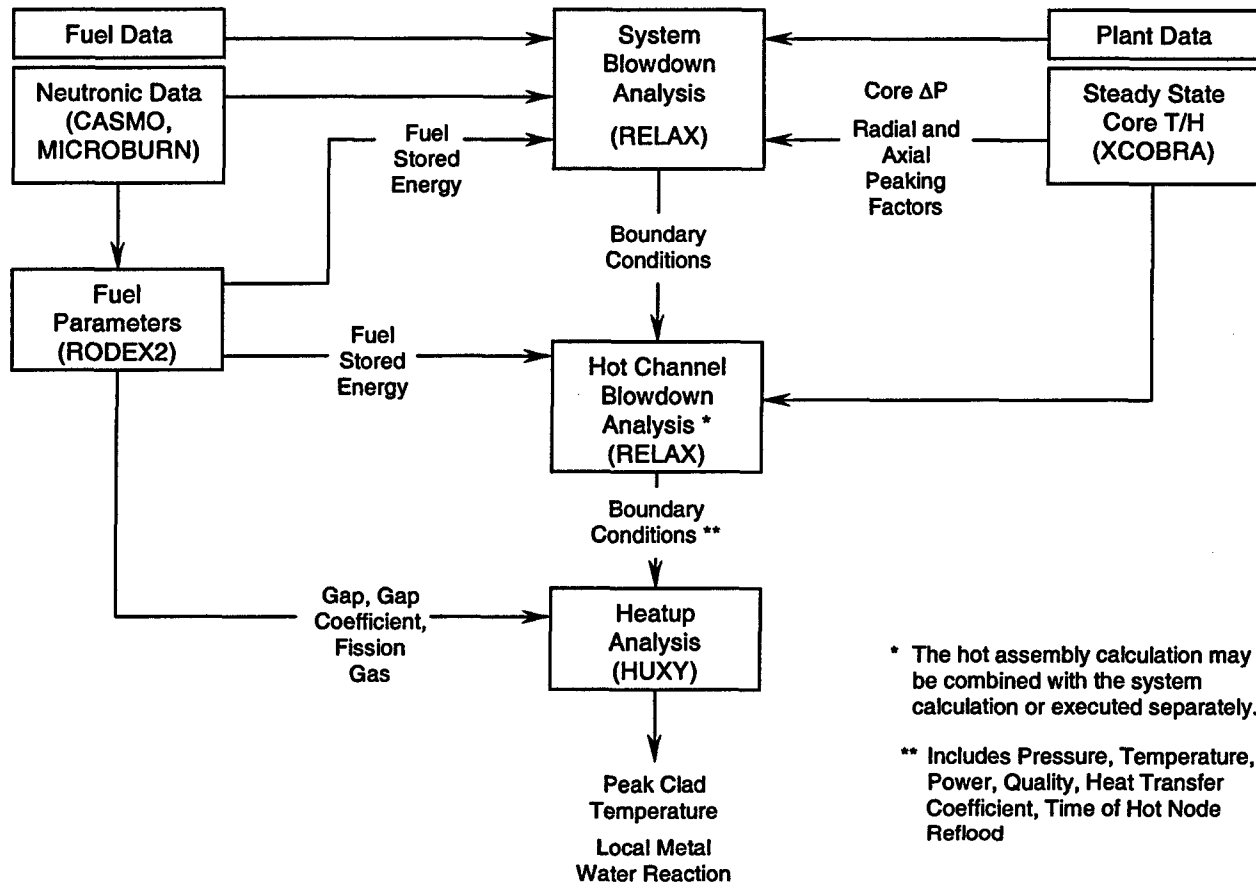


**Figure 3.6 LOCA-ECCS Calculation Process**

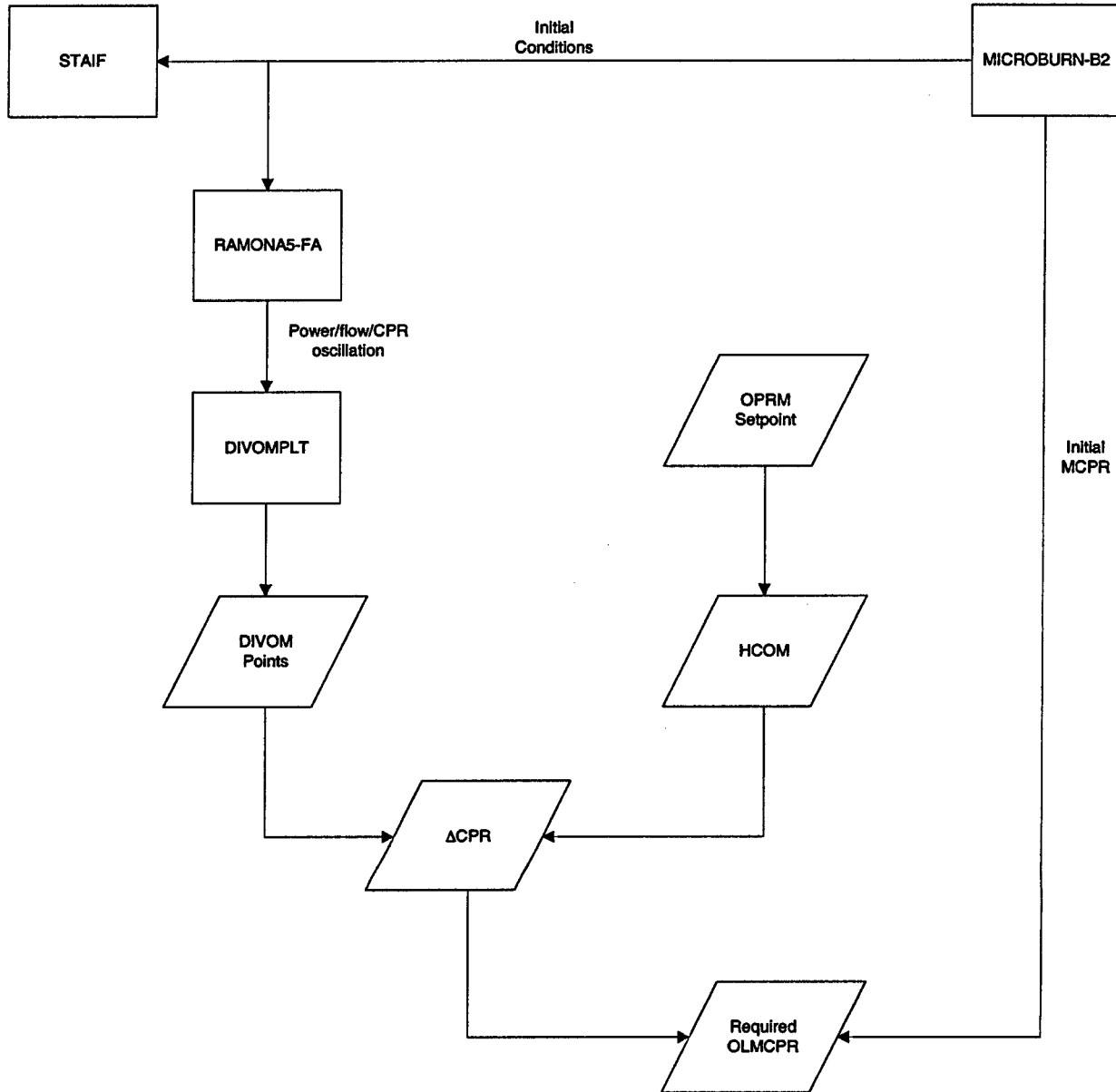


**Figure 3.7 Stability Calculation Process**

**NRC Question 4:**

(Nuclear Design): Provide plant and cycle specific information to show that the CASMO-4/MICROBURN-B2 code system was applied in a manner such that the predicted results for SSES 1 and 2 constant pressure power uprate analysis were within the range of the measurement uncertainties presented in EMF-2158(P)-A, "Siemens Power Corporation Methodology for Boiling Water Reactors: Evaluation and Validation of CASMO-4/MICROBURN-B2."

**PPL Response:**

CASMO-4 performs a multi-group [ ] spectrum calculation using a detailed heterogeneous description of the fuel lattice components. Fuel rods, absorber rods, water rods/channels and structural components are modeled explicitly. The library has cross sections for [ ] materials including [ ] heavy metals. Depletion is performed with a predictor-corrector approach in each fuel or absorber rod. The two-dimensional transport solution is based upon the [ ]. The solution provides pin-by-pin power and exposure distributions, homogeneous multi-group (2) microscopic cross sections as well as macroscopic cross sections. Discontinuity factors are determined from the solution. [ ] gamma transport calculation are performed. The code has the ability to perform [ ] calculation with different mesh spacings. Reflector calculations are easily performed.

MICROBURN-B2 performs microscopic fuel depletion on a nodal basis. The neutron diffusion equation is solved with a full two energy group method. Modern nodal method solution using discontinuity factors is used along with a [ ]. The flux discontinuity factors are [ ]. A multilevel iteration technique is employed for efficiency. MICROBURN-B2 treats a total of [ ] heavy metal nuclides to account for the primary reactivity components. Models for nodal [ ] are used to improve the accurate representation of the in-reactor configuration. Full three-dimensional pin power reconstruction method is utilized. TIP (neutron and gamma) and LPRM response models are included to compare calculated and measured instrument responses. Modern steady-state thermal-hydraulics models define the flow distribution among the assemblies. [ ] based upon CASMO-4 calculations are used for the in-channel fluid conditions as well as in the bypass and water rod regions. Modules for the calculation of CPR, LHGR, and MAPLHGR are implemented for direct comparisons to the operating limits.

MICROBURN-B2 determines the nodal macroscopic cross sections by summing the contribution of the various nuclides.

$$\Sigma_x(\rho, \Pi, E, R) = \sum_{i=1}^I N_i \sigma_x^i(\rho, \Pi, E, R) + \Delta \Sigma_x^b(\rho, \Pi, E, R)$$

where:

$\Sigma_x$	=	nodal macroscopic cross section
$\Delta\Sigma_x^b$	=	background nodal macroscopic cross section ( $D, \Sigma_f, \Sigma_a, \Sigma_r$ )
$N_i$	=	nodal number density of nuclide "i"
$\sigma_x^i$	=	microscopic cross section of nuclide "i"
$I$	=	total number of explicitly modeled nuclides
$\rho$	=	nodal instantaneous coolant density
$\Pi$	=	nodal spectral history
$E$	=	nodal exposure
$R$	=	control fraction

Functional representation of  $\sigma_x^i$  and  $\Delta\Sigma_x^b$  comes from three void depletion calculations with CASMO-4. Instantaneous branch calculations at alternate conditions of void and control state are also performed. The result is a multi-dimensional table of microscopic and macroscopic cross sections that is shown in Figure 4.1 and Figure 4.2.

At BOL the relationship is fairly simple, the cross section is only a function of void fraction (water density) and the reason for the variation is the change in the spectrum due to the water density variations. At any exposure point, a quadratic fit of the three CASMO-4 data points is used to represent the continuous cross section over instantaneous variation of void or water density. This fit is shown in Figure 4.3 and Figure 4.4.

Detailed CASMO-4 calculations confirm that a quadratic fit accurately represents the cross sections as shown in Figure 4.5, Figure 4.6, and Figure 4.7.

With depletion, the isotopic changes cause other spectral changes. Cross sections change due to the spectrum changes. Cross sections also change due to self-shielding as the concentrations change. These are accounted for by the void (spectral) history and exposure parameters. Exposure variations utilize a piecewise linear interpolation over tabulated values at [ ] exposure points. The four-dimensional representation can be reduced to three dimensions (see Figure 4.8) by looking at a single exposure.

Quadratic interpolation is performed in each direction independently for the most accurate representation. Considering the case at 70 GWd/MTU with an instantaneous void fraction of 70% and a historical void fraction of 60% Figure 4.9 and Figure 4.10 illustrate the interpolation process. The table values

from the library at 0, 0.40, and 0.80 void fractions are used to generate three quadratic curves representing the behavior of the cross section as a function of the historical void fraction for each of the tabular instantaneous void fractions (0, 0.40, and 0.80).

The intersection of the three quadratic lines with the historical void fraction of interest are then used to create another quadratic fit in order to obtain the resultant cross section as shown in Figure 4.10.

The results of this process for all isotopes and all cross sections in MICROBURN-B2 were compared for an independent CASMO-4 calculation with continuous operation at 40% void (40% void history) and branch calculations at 90% void for multiple exposures. The results show very good agreement for the whole exposure range as shown in Figure 4.11 and Figure 4.12.

At the peak reactivity point multiple comparisons were made (Figure 4.13) to show the results for various instantaneous void fractions.

Use of higher void fractions in CASMO-4 (for example: 0, 45, 90) introduces more error for intermediate void fractions. Figure 4.14 shows the difference between a 0, 40, 80 and a 0, 45, 90 interpolation method. Considering the better accuracy of the 0, 40, 80 methodology for the majority of assemblies (less than 85% void), the current methodology (0, 40, 80) is considered appropriate for current and CPPU conditions.

Void fraction has been used for the previous illustrations; however, MICROBURN-B2 uses water density rather than void fraction in order to account for pressure changes as well as sub-cooled density changes. This transformation does not change the basic behavior as water density is proportional to void fraction. MICROBURN-B2 uses spectral history rather than void history in order to account for other spectral influences due to actual core conditions (fuel loading, control rod inventory, leakage, etc.) The Doppler feedback due to the fuel temperature is modeled by accumulating the Doppler broadening of microscopic cross sections of each nuclide.

$$\left[ \Delta \Sigma_x = (\sqrt{T_{eff}} - \sqrt{T_{ref}}) \sum_i \frac{\partial \sigma_x^i}{\partial \sqrt{T_i}} N_i \right]$$

where:

$T_{eff}$  = Effective Doppler fuel temperature

$T_{ref}$  = Reference Doppler fuel temperature

$\sigma_x^i$  = Microscopic cross section (fast and thermal absorption) of nuclide  $i$

$N_i$  = Density of nuclide  $i$

The partial derivatives are determined from branch calculations performed with CASMO-4 at various exposures and void fractions for each void history depletion. The tables of cross sections include data for [ ] states. The process is the same for [ ] states. Other important feedbacks to nodal cross sections are lattice [ ] and instantaneous [ ] between lattices of different [ ]. These feedbacks are modeled in detail.

The methods used in CASMO-4 are state of the art. The methods used in MICROBURN-B2 are state of the art. The methodology accurately models a wide range of thermal hydraulic conditions including CPPU and reduced flow conditions.

The development of the void fraction correlation and the associated uncertainties are described below.

The Zuber-Findlay drift flux model (Reference 0) is utilized in the AREVA nuclear and safety analysis methods for predicting vapor void fraction in the BWR system. The model has a generalized form that may be applied to two-phase flow by defining an appropriate correlation for the void concentration parameter,  $C_o$ , and the drift flux,  $V_{gj}$ . The model parameters account for the radially non-uniform distribution of velocity and density and the local relative velocity between the phases, respectively. This model has received broad acceptance in the nuclear industry and has been successfully applied to a host of different applications, geometries, and fluid conditions through the application of different parameter correlations (Reference 4.2).

Two different correlations are utilized at AREVA to describe the drift flux parameters for the analysis of a BWR core. The correlations and treatment of uncertainties are as follows:

- The nuclear design, frequency domain stability, nuclear AOO transient, and accident analysis methods use the [ ] void correlation (Reference 0) to predict nuclear parameters. Uncertainties are addressed at the overall methodology and application level rather than individually for the individual correlations of each method. The overall uncertainties are determined statistically by comparing predictions using the methods against measured operating data for reactors operating throughout the world.

- The thermal-hydraulic design, system AOO transient and accident analysis, and loss of coolant accident (only at specified junctions) methods use the Ohkawa-Lahey void correlation (Reference 0). This correlation is not used in the direct computation of nuclear parameters in any of the methods. Uncertainties are addressed at the overall methodology level through the use of conservative assumptions and biases to assure uncertainties are bounded.

The [ ] void correlation was developed for application to multi-rod geometries operating at typical BWR operating conditions using multi-rod data and was also validated against simple geometry data available in the public domain. The correlation was defined to be functionally dependent on the mass flux, hydraulic diameter, quality, and fluid properties.

The multi-rod database used in the [

]. As a result, the multi-rod database and prediction uncertainties are not available to AREVA. However, the correlation has been independently validated by AREVA against public domain multi-rod data and proprietary data collected for a prototypical ATRIUM-10 test assembly. Selected results for the ATRIUM-10 test assembly are reported in the public domain in Reference 4.5.

The Ohkawa-Lahey void correlation was developed for application in BWR transient calculations. In particular, the correlation was carefully designed to predict the onset of counter current flow limit (CCFL) characteristics during the occurrence of a sudden inlet flow blockage. The correlation was defined to be functionally dependent on the mass flux, quality, and fluid properties.

Independent validation of the correlation was performed by AREVA at the request of the NRC during the review of the XCOBRA-T code. The NRC staff subsequently reviewed and approved Reference 0, which compared the code to a selected test from the FRIGG experiments (Reference 0). More recently, the correlation has been independently validated by AREVA against additional public domain multi-rod data and proprietary data collected for a prototypic ATRIUM-10 test assembly.

The characteristics of the AREVA multi-rod void fraction validation database are listed in Table 4.1.

The FRIGG experiments have been included in the validating database because of the broad industry use of these experiments in benchmarking activities, including TRAC, RETRAN and S-RELAP5. The experiments include a wide range of pressure, subcooling, and quality from which to validate the general applicability of a void correlation. However, the experiments do not contain features found in

modern rod bundles such as part length fuel rods and mixing vane grids. The lack of such features makes the data less useful in validating correlations for modern fuel designs. Also, the reported instrument uncertainty for these tests is provided in Table 4.1 based on mockup testing. However, the total uncertainty of the measurements (including power and flow uncertainties) is larger than the indicated values.

Because of its prototypical geometry, the ATRIUM-10 void test data was useful in validating void correlation performance in modern rod bundles that include part length fuel rods, mixing vane grids, and prototypic axial/radial power distributions. Void measurements were made at one of three different elevations in the bundle for each test point: just before the end of the part length fuel rods, midway between the last two spacers, and just before the last spacer.

As shown in Figure 4.15, the range of conditions for the void data for typical reactor conditions are enveloped by the ATRIUM-10 void fraction test data except for the high flow/low exit quality data. This figure compares the equilibrium quality at the plane of measurement for the ATRIUM-10 void data with the exit quality of bundles in the EMF-2158 benchmarks and SQH operating at CPPU (including reduced flow) conditions. As seen in the figure, the SQH operating data is enveloped by the EMF-2158 benchmarks.

Figure 4.16 and Figure 4.17 provide comparisons of predicted versus measured void fractions for the AREVA multi-rod void fraction validation database using the [ ] correlation. These figures show the predictions fall within  $\pm 0.05$  (predicted – measured) error bands with good reliability and with very little bias. Also, there is no observable trend of uncertainty as a function of void fraction.

Figure 4.18 and Figure 4.19 provide comparisons of predicted versus measured void fractions for the AREVA multi-rod void fraction validation database using the Ohkawa-Lahey correlation. In general, the correlation predicts the void data with a scatter of about  $\pm 0.05$  (predicted – measured), but a bias in the prediction is evident for voids between 0.5 and 0.8. The observed under prediction is consistent with the observations made in Reference 4.6.

In conclusion, validation using the AREVA multi-rod void fraction validation database has shown that both drift flux correlations remain valid for modern fuel designs. Furthermore, there is no observable trend of uncertainty as a function of void fraction. This shows there is no increased uncertainty in the prediction of nuclear parameters at CPPU (including reduced flow) conditions within the nuclear methods as a result of changes to the population distribution of the nodal void fractions with respect to pre CPPU conditions.

AREVA has reviewed the data presented in EMF-2158(P)(A) with regard to the maximum assembly power (Figure 4.20) and maximum exit void fraction (Figure 4.21) to determine the range of data previously benchmarked.

Actual operating data from several recent fuel cycle designs have also been evaluated and compared to that in the topical report EMF-2158(P)(A). Maximum assembly powers and maximum void fractions similar to that presented above are presented in Figure 4.22 and Figure 4.23.

In order to evaluate some of the details of the void distribution, a current design calculation was reviewed in more detail. Figure 4.24 and Figure 4.25 present the following parameters at the point of the highest exit void fraction (at 9336 MWd/MTU cycle exposure) in cycle core design for a BWR-6 reactor with ATRIUM-10 fuel. These are representative figures for a high power density plant and do not correspond to the data from Figure 4.22 and Figure 4.23.

- Core average axial void profile
- Axial void profile of the peak assembly
- Histogram of the nodal void fractions in core

The EMF-2158(P)(A) data was also re-evaluated by looking at the deviations between measured and calculated Traversing Incore Probe (TIP) response for each axial level. The standard deviation of these deviations at each axial plane are presented in Figure 4.26 and demonstrates that there is no significant trend versus axial position, which indicates no significant trend versus void fraction.

Gamma scan comparisons for 9x9-1 and ATRIUM-10 fuel were presented in the topical report, EMF-2158(P)(A), in Section 8.2.2. Figures 8.18 through 8.31 in this document show very good comparisons between the calculated and measured relative Ba-140 density distributions for both radial and axial values.

Pin-by-pin gamma scan data is used for verification of the local peaking factor uncertainty. Quad Cities 1 measurements presented in the topical report EMF-2158(P)(A) have been re-evaluated to determine any axial dependency. Figure presents the raw data including measurement uncertainty and demonstrates that there is no axial dependency. The more recent gamma scans performed by



Fuel loading patterns and operating control rod patterns are constrained by the MCPR limit, which consequently limits the assembly power and exit void fraction regardless of the core power level. The axial profile of the power and void fraction of the limiting assembly and core average values are presented in Figure 4.30 for the Susquehanna CPPU cycle design. This data corresponds to the maximum exit void fraction experienced throughout the CPPU design cycle.

Another measure of the thermal-hydraulic conditions is the population distribution of the void fractions.

Figure 4.31 presents a histogram of the void fraction for CPPU conditions. This histogram was taken at the point of maximum exit void fraction expected during the cycle. The population of nodes experiencing 85 to 90% voids is relatively small.

Reactor conditions for Susquehanna with power uprate are not significantly different from that of current experience. The range of void fractions in the topical report data exceeds that expected for the power uprate conditions. The distribution of voids is nearly the same as current experience.

Data presented in these figures and tables demonstrate that the AREVA methodology is capable of accurately predicting reactor conditions for fuel designs operated under CPPU operating strategies and core conditions and SSES 1 and 2 CPPU analysis are within the range of measurement uncertainties presented in EMF-2158 (P)(A).

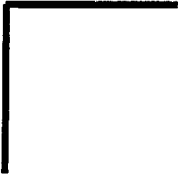
**References:**

- 4.1 N. Zuber and J.A. Findlay, "Average Volumetric Concentration in Two-Phase Flow Systems," *J. Heat Transfer*, pp. 453–468, November 1965 .
- 4.2 P. Coddington and R. Macian, "A Study off the Performance of Void Fraction Correlations Used In the Context of Drift-Flux Two-Phase Flow Models," *Nuclear Engineering and Design*, 215, 199–216.
- 4.3 [ ]
- 4.4 K. Ohkawa and R. T. Lahey Jr., "The Analysis of CCFL Using Drift-Flux Models," *Nuclear Engineering and Design*, 61, 1980.
- 4.5 S. Misu et al., "The Comprehensive Methodology for Challenging BWR Fuel Assembly and Core Design used at Framatome ANP," proceedings on CD-ROM, PHYSOR 2002, Seoul, South Korea, October 7-10, 2002.
- 4.6 XN-NF-84-105(P)(A) Volume 1 Supplement 4, *XCOBRA-T: A Computer Code for BWR Transient Thermal-Hydraulic Core Analysis - Void Fraction Model Comparison to Experimental Data*, Advanced Nuclear Fuels Corporation, June 1988.
- 4.7 O. Nylund et al., "Hydrodynamic and Heat Transfer Measurements on A Full-Scale Simulated 36-Rod Marviken Fuel Element with Non-Uniform Radial Heat Flux Distribution," FRIGG-3, R-494/RL-1154, November 1969.
- 4.8 J. Skaug et al., "FT-36b, Results of void Measurements," FRIGG-PM-15, May 1968.
- 4.9 O. Nylund et al., "Hydrodynamic and Heat Transfer Measurements on a Full-Scale Simulated 36-Rod Marviken Fuel Element With Uniform Heat Flux Distribution," FRIGG-2, R-447/RTL-1007, May 1968.
- 4.10 A1C-1308656-1, "Initial Void Measurements at the Karlstein Thermal Hydraulic Test Loop," AREVA NP, April 2003.
- 4.11 EMF-85-74(P) Revision 0 Supplement 1(P)(A) and Supplement 2(P)(A), *RODEX2A (BWR) Fuel Rod Thermal-Mechanical Evaluation Model*, Siemens Power Corporation, February 1998.

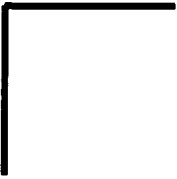
**Table 4.4 AREVA Multi-Rod Void  
Fraction Validation Database**

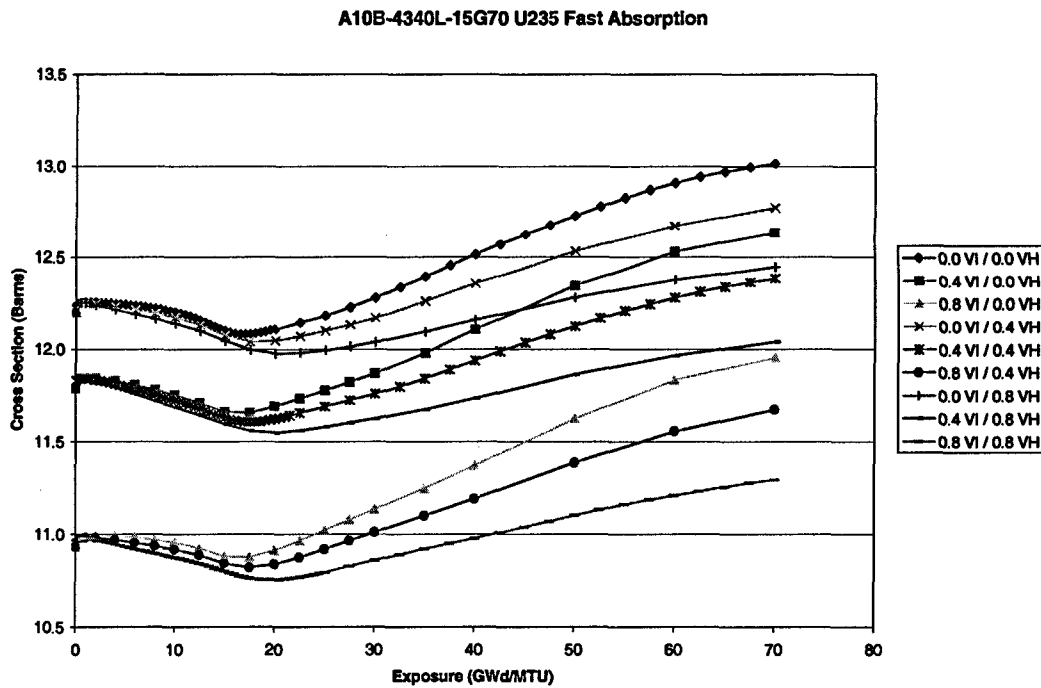
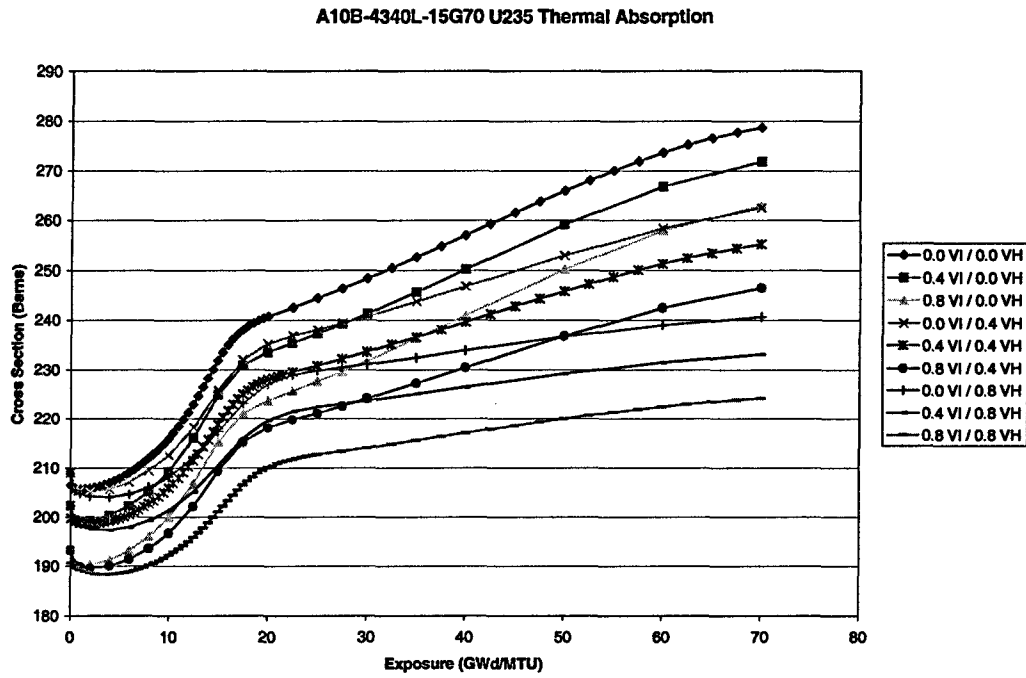
	FRIGG-2 (Reference 4.9)	FRIGG-3 (References 4.7 and 4.8)	ATRIUM-10- KATHY (Reference 4.10)
Axial Power Shape	uniform	uniform	[ ]
Radial Power Peaking	uniform	mild peaking	[ ]
Bundle Design	circular array with 36 rods + central thimble	circular array with 36 rods + central thimble	prototypic ATRIUM-10 CHF bundle
Pressure (psi)	725	725, 1000, and 1260	[ ]
Inlet Subcooling ( <sup>0</sup> F)	4.3 to 40.3	4.1 to 54.7	[ ]
Mass Flow Rate (lbm/s) <i>(calculated from mass flux assuming ATRIUM-10 inlet flow area)</i>	14.3 to 31.0	10.1 to 42.5	[ ]
Equilibrium Quality at Measurement Plane (fraction)	-0.036 to 0.203	-0.058 to 0.330	[ ]
Max Void at Measurement Plane (fraction)	0.828	0.848	[ ]
Reported Instrument Uncertainty (fraction)	0.025	0.016	[ ]
Number of Data	27 tests, 174 points	39 tests, 157 points	[ ]

**Table 4.5 KWU-S Gamma Scan Benchmark  
Results From EMF-2158(P)(A)**



**Table 4.6 Comparison of CASMO-4 and  
MCNP Results for ATRIUM-10 Design**





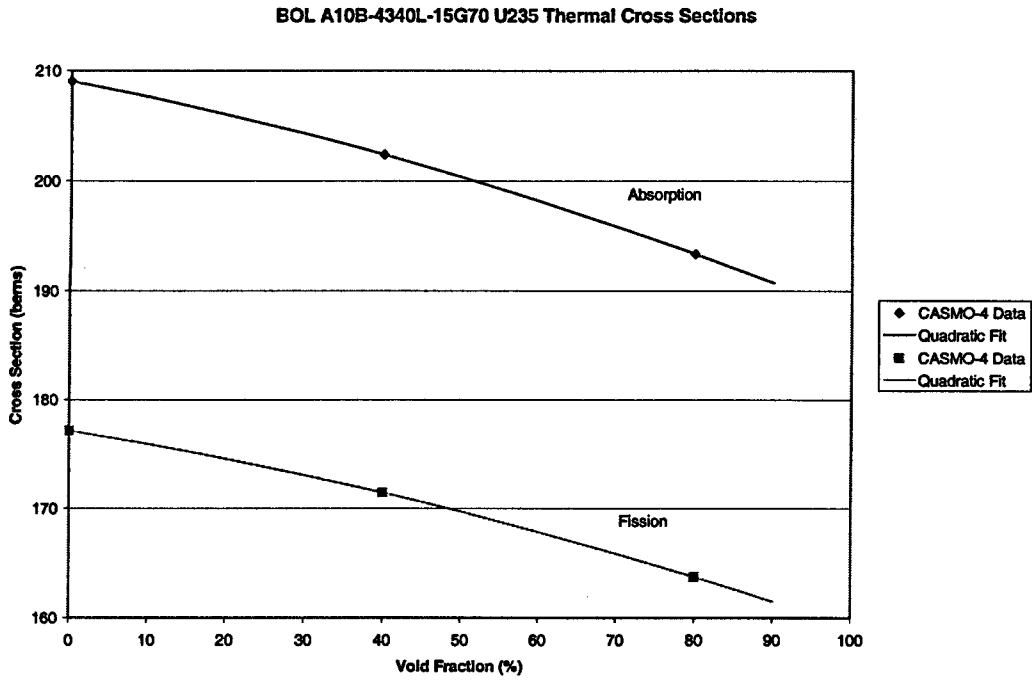


**Figure 4.3 Microscopic Thermal Cross Section of U-235 at Beginning of Life**

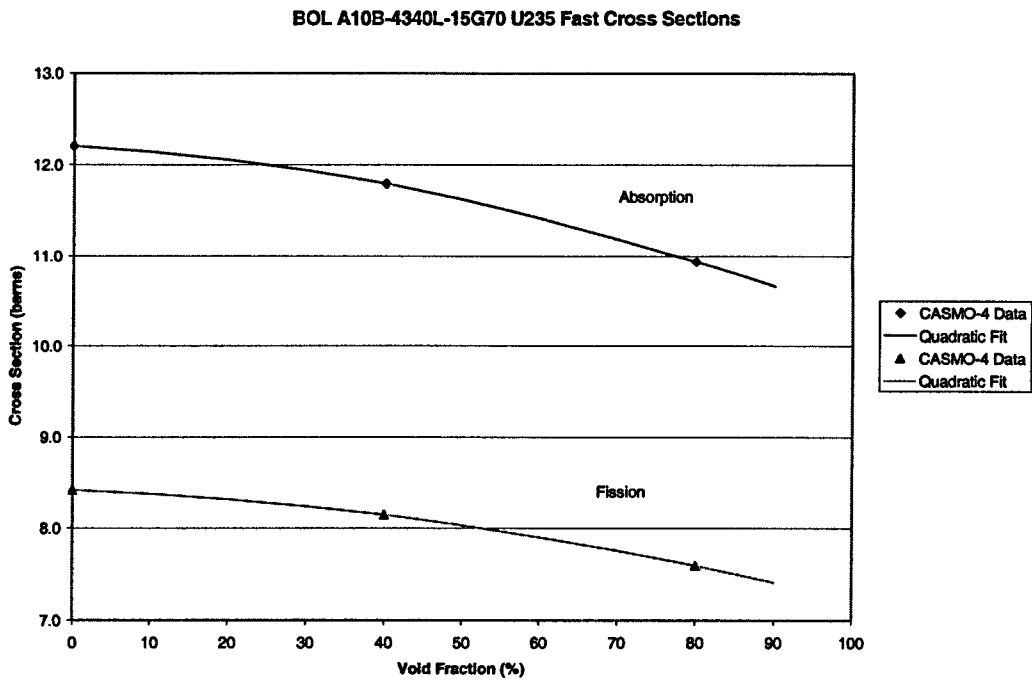


**Figure 4.4 Microscopic Fast Cross Section of U-235 at Beginning of Life**

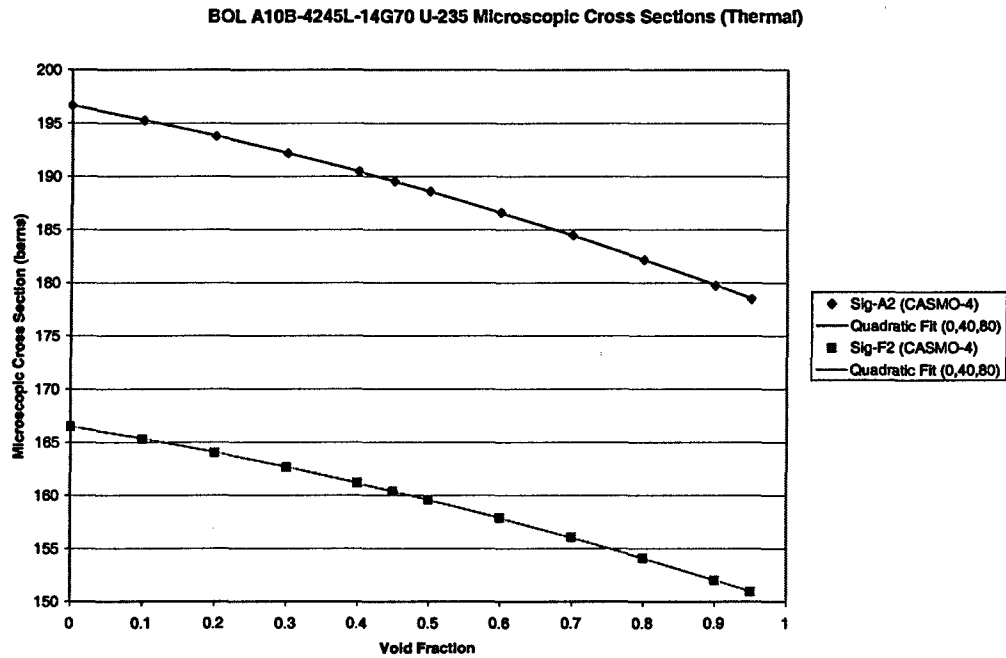


**Figure 4.5 Microscopic Thermal Cross Section of U-235 Comparison of Quadratic Fit With Explicit Calculations at Various Void Fractions**

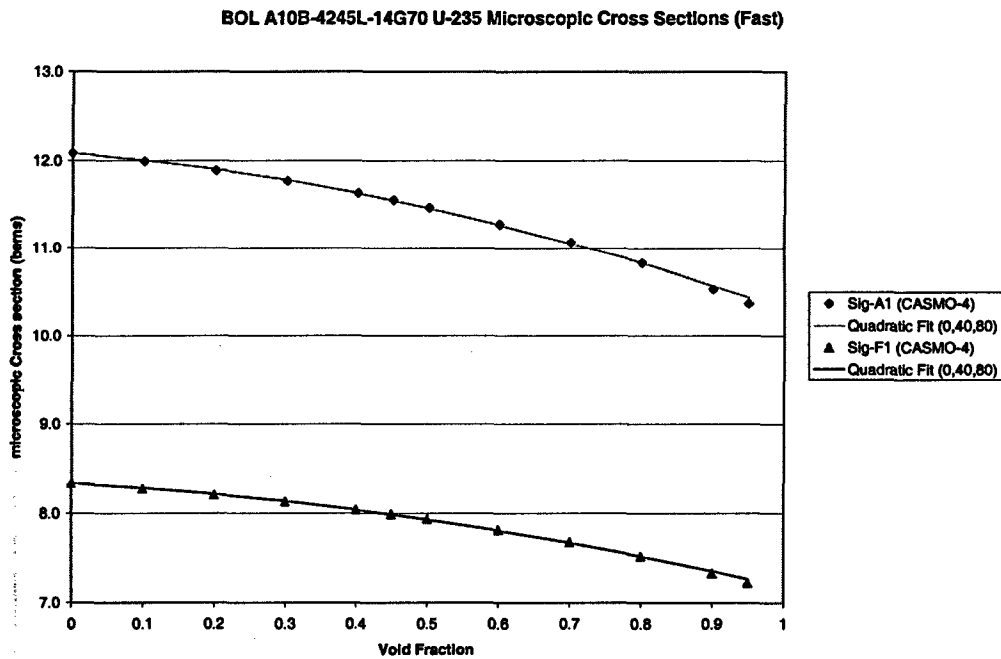


**Figure 4.6 Microscopic Fast Cross Section of U-235 Comparison of Quadratic Fit With Explicit Calculations at Various Void Fractions**

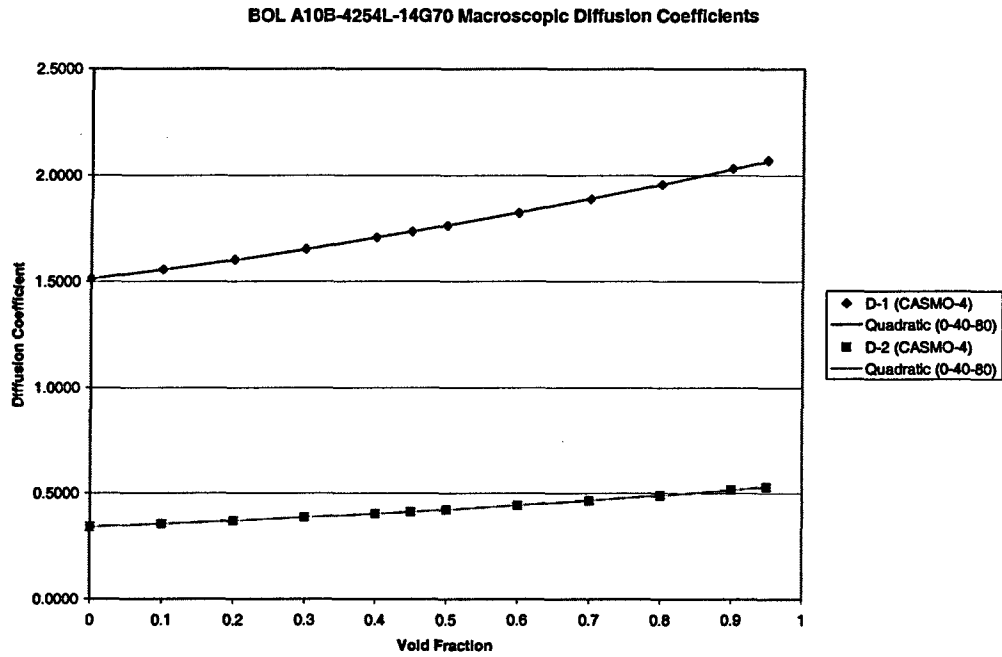


**Figure 4.7 Macroscopic Diffusion Coefficient (Fast and Thermal) Comparison of Quadratic Fit With Explicit Calculations at Various Void Fractions**

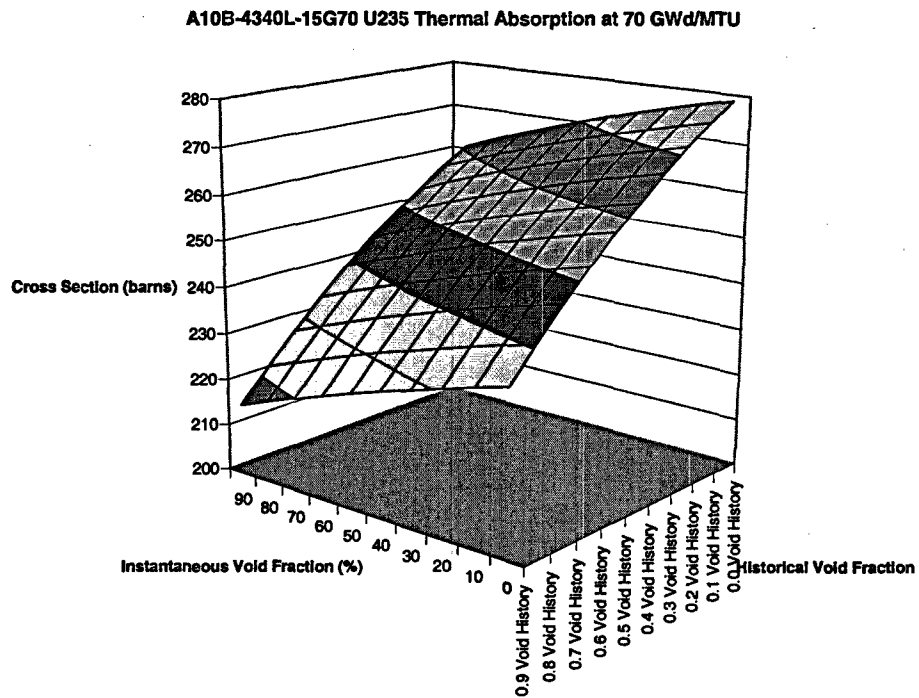


**Figure 4.8 Microscopic Thermal Cross Section of U-235 at 70 GWd/MTU**

A10B-4340L-15G70 U235 Thermal Absorption at 70 GWd/MTU

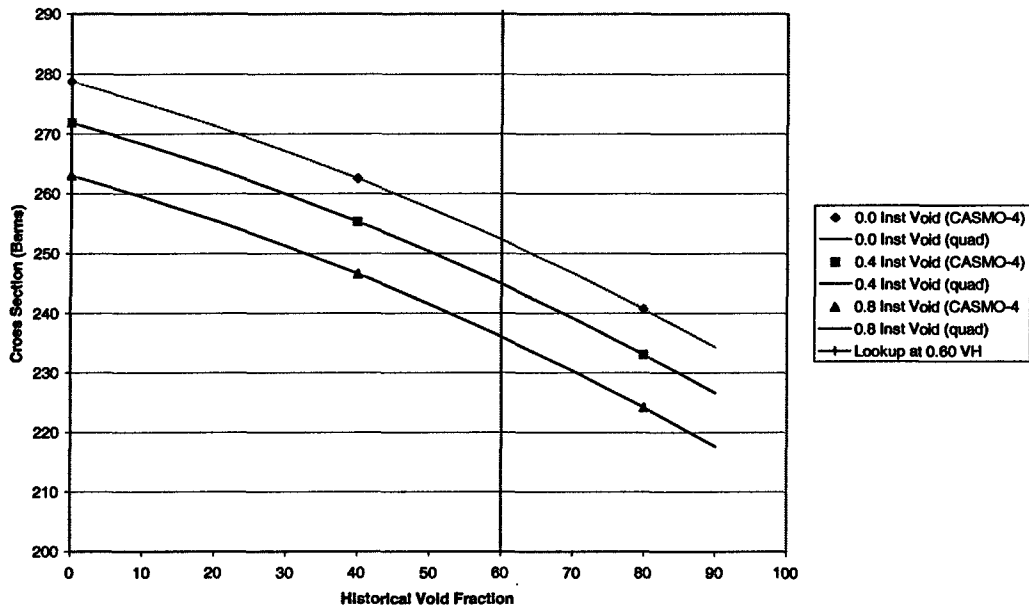


Figure 4.9 Quadratic Interpolation Illustration of Microscopic Thermal Cross Section of U-235

A10B-4340L-15G70 U235 Thermal Absorption at 70 GWd/MTU

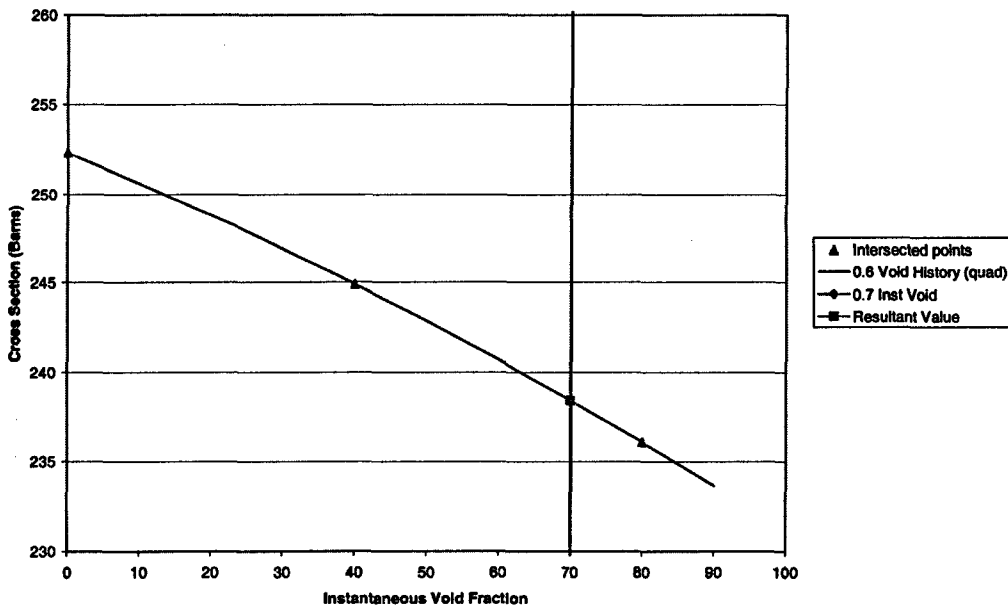
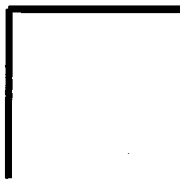


Figure 4.10 Illustration of Final Quadratic Interpolation for Microscopic Thermal Cross Section of U-235



**Figure 4.11 Comparison of k-inf From MICROBURN-B2 Interpolation Process With CASMO-4 Calculations at Intermediate Void Fractions of 0.2, 0.6, and 0.9**



**Figure 4.12 Comparison of k-inf From MICROBURN-B2 Interpolation Process With CASMO-4 Calculations at 0.4 Historical Void Fractions and 0.9 Instantaneous Void Fraction**



**Figure 4.13 Delta k-inf From MICROBURN-B2 Interpolation Process With CASMO-4 Calculations at 0.4 Historical Void Fraction and 0.9 Instantaneous Void**

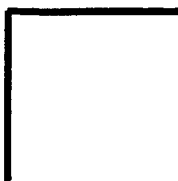


**Figure 4.14 Comparison of Interpolation Process Using Void Fractions of 0.0, 0.4, and 0.9 and Void Fractions of 0.0, 0.45, and 0.9**

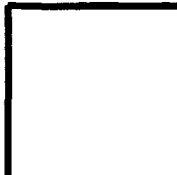


**Figure 4.15 Comparison of the Measured Local Quality for ATRIUM-10  
Void Data and Exit Quality for Typical Reactor Conditions**

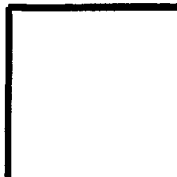


**Figure 4.16 Validation of [ ] Using  
FRIGG-2 and FRIGG-3 Void Data**

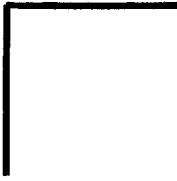


**Figure 4.17 Validation of [ ] Using  
ATRIUM-10 Void Data**

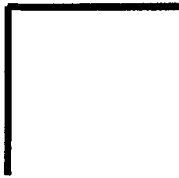


**Figure 4.18 Validation of Ohkawa-Lahey Using  
FRIGG-2 and FRIGG-3 Void Data**

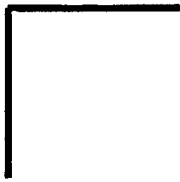


**Figure 4.19 Validation of Ohkawa-Lahey Using  
ATRIUM-10 Void Data**



**Figure 4.20 Maximum Assembly Power in  
Topical Report EMF-2158(P)(A)**



**Figure 4.21 Maximum Exit Void Fraction in  
Topical Report EMF-2158(P)(A)**

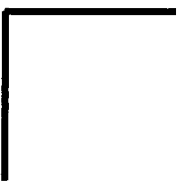


**Figure 4.22 Maximum Assembly Power Observed From  
Recent Operating Experience**

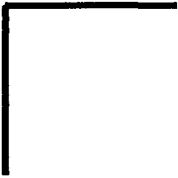


**Figure 4.23 Void Fractions Observed From Recent Operating Experience**

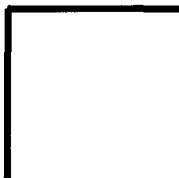


**Figure 4.24 Axial Power and Void Profile Observed From Recent Design Experience**

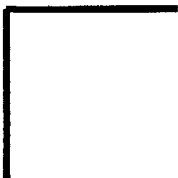


**Figure 4.25 Nodal Void Fraction Histogram Observed From Recent Design Experience**

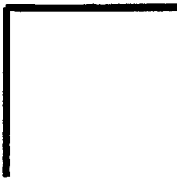


**Figure 4.26 EMF-2158(P)(A) TIP Statistics by Axial Level**

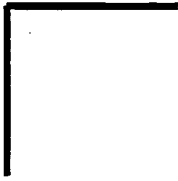


**Figure 4.27 Quad Cities Unit 1  
Pin-by-Pin Gamma Scan Results**

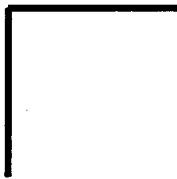


**Figure 4.28 Maximum Assembly Power in the  
Susquehanna Design**



**Figure 4.29 Maximum Exit Void Fraction in the Susquehanna Design**

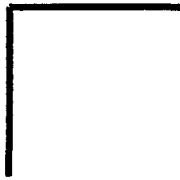


**Figure 4.30 Axial Power and Void Profile for Susquehanna CPPU Design**



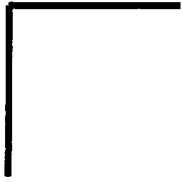


**Figure 4.31 Susquehanna CPPU Nodal Void Fraction Histogram**

**NRC Question 8:**

(Thermal and Hydraulic Design): Demonstrate that the statistical process used to determine the safety limit minimum critical power ratio is both statistically rigorous and conservative enough to be applied to the flatter radial power distribution required to achieve CPPU. For the limiting operating state point, characterize the Monte Carlo distribution of safety limit minimum critical power ratio values in terms of the shape of the distribution, its upper and lower tolerance limits, and the number of runs required to develop a 95% confidence level.

**PPL Response 8:**

The statistical process used in the Safety Limit Methodology is described in the topical report ANF-524(P)(A) Revision 2 and Supplements 1 and 2. This process uses a statistical convolution of the uncertainties associated with the calculation of thermal margin for the determination of the safety limit MCPR – the limit for which at least 99.9% of the rods in the core are expected to avoid boiling transition. In accordance with Section 4.4 of NUREG-800, the approach that may be used to meet the criteria of the SRP is:

For DNBR, CHF<sub>R</sub> or CPR correlations, the limiting (minimum) value of DNBR, CHF<sub>R</sub>, or [ ] CPR is to be established such that at least 99.9% of the fuel rods in the core would not be expected to experience departure from nucleate boiling or boiling transition during normal operation or anticipated operational occurrences.

This is the approach that is used in the safety limit methodology and is the approach that is approved by the SER for the safety limit methodology. The uncertainties associated with the calculation of MCPR include both fuel-related uncertainties, which may vary with reactor loading cycle, and non-fuel-related uncertainties, which are characteristics of the reactor system.

Non-fuel-related uncertainties are those uncertainties which do not depend upon the particular type of fuel present in the reactor core. Examples of non-fuel-related uncertainties are the measurement uncertainties associated with reactor pressure, feedwater flow rate and temperature and total core flow. The accuracy of these measured values depends on the plant instrumentation and the uncertainties used in the safety limit MCPR calculations are provided to AREVA by the responsible utility. [

]

The uncertainties used in determining the MCPR safety limit are statistically convolved via a Monte Carlo procedure. The Monte Carlo procedure simulates a variety of reactor states around a base state (nominal conditions) where the core MCPR is equal to the MCPR safety limit. [







**Figure 8.1 Stratification Technique Employed in Monte Carlo Perturbation Process**



**Figure 8.2 Typical Mean Number of  
Rods in BT During 1000 Trials**

**The following provides the supplemental information NRC requested be provided in a teleconference call between PPL and the NRC Staff held on June 6, 2007.**

**NRC Supplemental Question 1:**

The NRC staff would like to confirm that the Susquehanna small break LOCA PCT result is not limiting compared to large break LOCA result. Specifically, the NRC staff requests PPL to provide the following information for the most limiting small break LOCA case (SF-BATT, 0.7 ft2 split, top peak, pump discharge break).

- 1.1. Plant initial condition, axial power shape, radial peaking and local peaking factors.
- 1.2. Sequence of events.
- 1.3. Break size, ECCS flows and locations including HPCI, LPCI, LPCS and ADS.
- 1.4. Major parameter plots similar to large break LOCA results (Figure 6.1 to 6.27 in EMF-3242P)

**PPL Response 1.1:**

The requested, steady state initial conditions and radial peaking are summarized in Table A.1 and includes the values shown in Table 4.1 of EMF-3242(P), Rev. 0, Susquehanna LOCA Break Spectrum Analysis for ATRIUM<sup>TM-10</sup> Fuel and Extended Power Uprate, November 2005. The axial power shape is presented in Table A.2 and is based on the plot shown in Figure 4.5 of EMF-3242(P). The local peaking factors are presented in Table A.3. These results demonstrate that the Susquehanna small break LOCA PCT result is not limiting compared to the large break results provided in Reference 3.

**PPL Response 1.2:**

The requested sequence of events is provided in Table A.4.

**PPL Response 1.3:**

The break size is precisely 0.7 ft<sup>2</sup> in the piping connected to the recirculation pump discharge (PD). The break occurs during full power operation at the CPPU power stated in Table A.1, a core flow of 108 Mlbm/hr, and the top peaked axial power profile depicted in Figure 4.5 of EMF-3242(P). The single ECCS failure in this analysis is the DC power supply, designated SF-BATT. For a PD break with SF-BATT, the available ECCS are ADS, one of two LPCS systems, and one LPCI pump injecting into the intact loop. No HPCI flow is available for the SF-BATT scenario. Figure 4.2 of EMF-3242(P) shows the locations for fill junctions used to represent HPCI, LPCI, LPCS, and ADS in the RELAX model. Plots of the flow versus time for each of these systems are included in the set of parameter plots requested in NRC Question 3 of Reference 4.

**PPL Response 1.4:**

The requested parameter plots are shown in Figures A.1 to A.27.

**NRC Supplemental Question 2:**

Per page 2-1 of EMF-3242(P), the analyses for two-loop operation support a 5 Mlbm/hr mismatch in the recirculation jet pump loop flows at the start of the LOCA. Provide these loop flow values for top peak state points 108F and 80F.

**PPL Response:**

The requested flow rate values are shown in Table A.5.

**NRC Supplemental Question 3:**

Per Table 6.9 of EMF-3242(P), the limiting LOCA for two-loop operation and a core flow of 108 Mlbm/hr is the 0.8 DEG pump suction (PS) break with SF-LPCI and top peak. Provide the corresponding major parameter plots similar to Figure 6.1 to 6.27 in EMF-3242(P).

**PPL Response:**

The requested parameter plots are shown in Figures A.28 to A.54. Data provided in Tables A.1 through A.3 are also applicable to this break. Event times for the 0.8 DEG PS SF-LPCI TOP 108F break are shown in Table A.4.

**NRC Supplemental Question 4:**

Provide the LOCA reports that address the analysis performed for the currently licensed thermal power (CLTP) for the SSES units.

**PPL Response:**

The requested reports are EMF-3153(P), Rev. 3, "Susquehanna LOCA Break Spectrum Analysis for ATRIUM<sup>TM-10</sup> Fuel with EXEM BWR-2000 ECCS Evaluation Model", February 2006 (break spectrum) and EMF-3154(P), Rev. 2, "Susquehanna LOCA Analysis MAPLHGR Limit for ATRIUM<sup>TM-10</sup> Fuel with EXEM BWR-2000 Methodology", February 2006 (heatup) and in Attachment 4. The corresponding reports for CPPU are EMF-3242(P) (break spectrum) and EMF-3243(P), Rev. 0, "Susquehanna LOCA MAPLHGR Analysis for ATRIUM<sup>TM-10</sup> Fuel and Extended Power Uprate", November 2005 (heatup).

**NRC Supplemental Question 5:**

Provide the reference and/or description of the models governing counter-current flow (CCFL) at the exit to the hot bundle/core.

**PPL Response:**

In AREVA's NRC approved EXEM BWR-2000 methodology, CCFL is calculated for the average core and hot channel regions independently using the Kutateladze Correlation (K. H. Sun and R. T. Fernandez, "Countercurrent Flow Limitation Correlation for BWR Bundles During LOCA," ANS Transactions, Vol. 27, Pages 605-606, 1977) which is included in Attachment 3. The Ohkawa-Lahey Drift Flux Model (K. Ohkawa and R. T. Lahey, Jr., "The Analysis of Proposed BWR Inlet Flow Blockage Experiments in PBF," NES-486, Rensselaer Polytechnic Institute, Troy, NY, December 1978) is used to calculate two-phase slip at junctions in the fuel bundle and collapses to the Kutateladze formulation at the CCFL limit which is included in Attachment 3. The use of these models is described further in Section 2 of XN-NF-80-19(P)(A) Volume 2A, included as part of XN-NF-80-19(P)(A), Volumes 2, 2A, 2B, and 2C, "Exxon Nuclear Methodology for Boiling Water Reactors EXEM BWR ECCS Evaluation Model, Exxon Nuclear Company, September 1982."

**Table A.1 Initial Conditions for  
TOP 108F Breaks**

Reactor power (% of rated)	102.0
Reactor power (MWt)	4031.0
Steam dome pressure (psia)	1054.1
Downcomer water level in the RPV, inches above vessel zero	562.5
above top of active fuel	196.7
Total core flow (Mlb/hr)	108.0
Feedwater flow rate (Mlb/hr)	16.9
Steam flow rate (Mlb/hr)	16.9
Recirculation loop flow (Mlb/hr) <sup>6</sup>	34.2
Core inlet enthalpy (Btu/lb)	523.8

<sup>6</sup> Includes both loops.

**Table A.2 Axial Power Shape for  
TOP 108F Breaks**

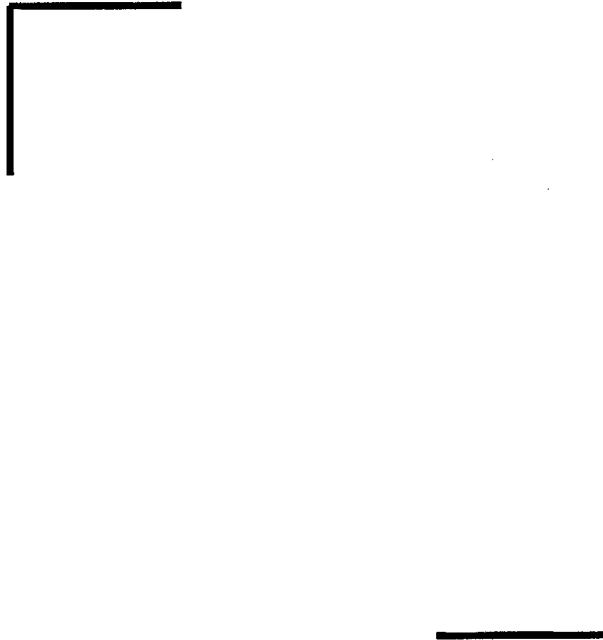


**Table A.3 Local Peaking Factors for  
TOP 108F Breaks**



**Table A.4 Event Times**

Event	0.7ft <sup>2</sup> split PD SF-BATT 108F TOP Time (sec)	0.8 DEG PS SF-LPCI 108F TOP Time (sec)
Initiate break, loss of offsite power	0.0	0.0
Initiate MSIV closure	2.0	2.0
Initiate scram (MSIV < 85% open)	2.5	2.5
MSIV fully closed	5.0	5.0
L2 low water level, HPCI signaled	12.7	6.1
L1 low water level, DG signaled	21.1	8.0
Jet pump suction uncovers	28.0	8.7
Recirc suction uncovers	43.2	11.6
Lower plenum flashes	51.8	14.0
DG power at ESS bus	46.2	33.1
HPCI flow starts	NA	40.2
LPCI pumps start	50.2	37.1
IL LPCI valve starts to open	153.8	NA
IL LPCI flow starts	165.4	NA
BL LPCI valve starts to open	NA	46.4
BL LPCI flow starts	NA	46.4
LPCS pump starts	57.7	44.6
LPCS valve starts to open	153.8	46.4
LPCS flow starts	159.7	48.1
ADS valve starts to open	141.1	128.0
RDIV closure starts	178.6	54.1
RDIV closure complete	211.6	87.1
Begin rated spray (TSPRAY)	208.6	69.3
End of blowdown	208.6	69.3
Bypass reflood	271.3	122.4
Core reflood	265.5	115.9
PCT	265.5	115.9

**Table A.5 Individual Recirculation Loop  
Flow Rates for TOP Peak**

	Initial Total Core Flow (Mlbm/hr)	
Initial Flow (Mlbm/hr) for:	108	80

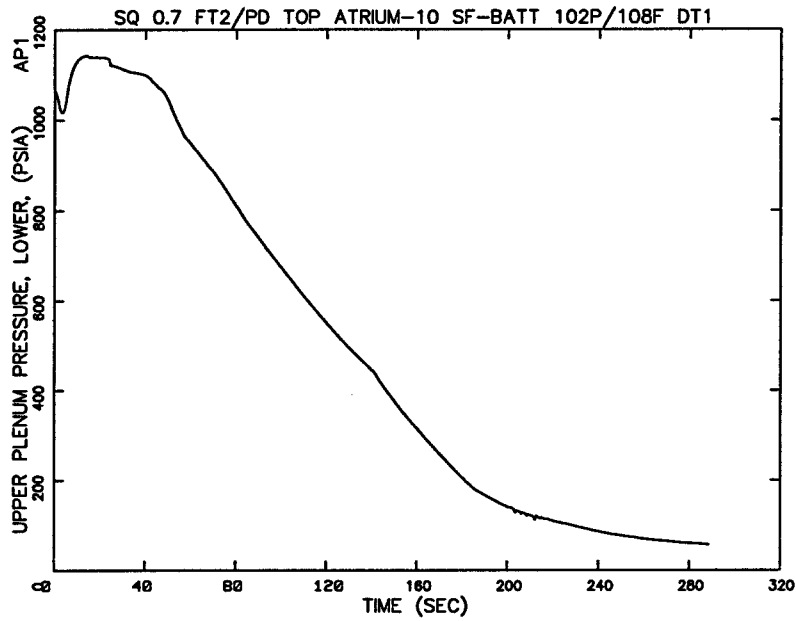


**Figure A.1 0.7 ft<sup>2</sup> PD SF-BATT TOP 108F  
Upper Plenum Pressure (Lower)**

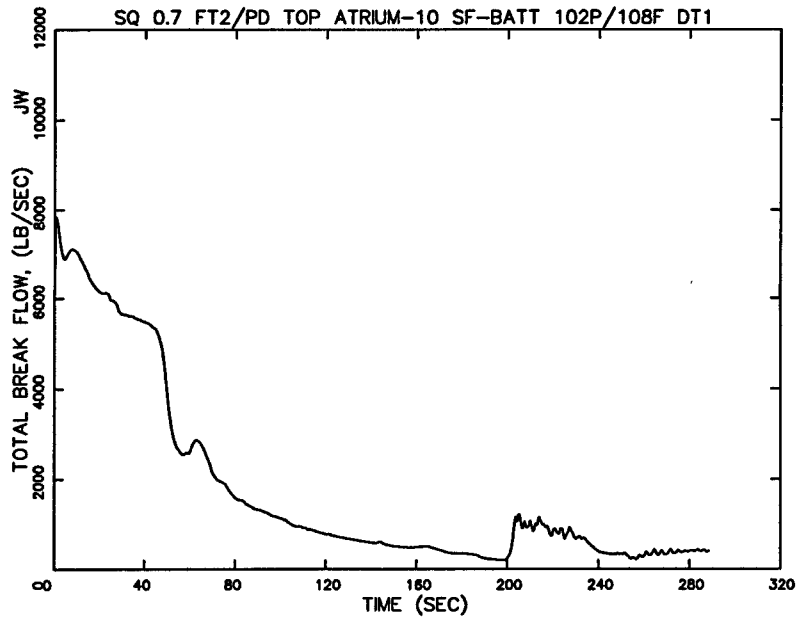


**Figure A.2 0.7 ft<sup>2</sup> PD SF-BATT TOP 108F  
Total Break Flow Rate**

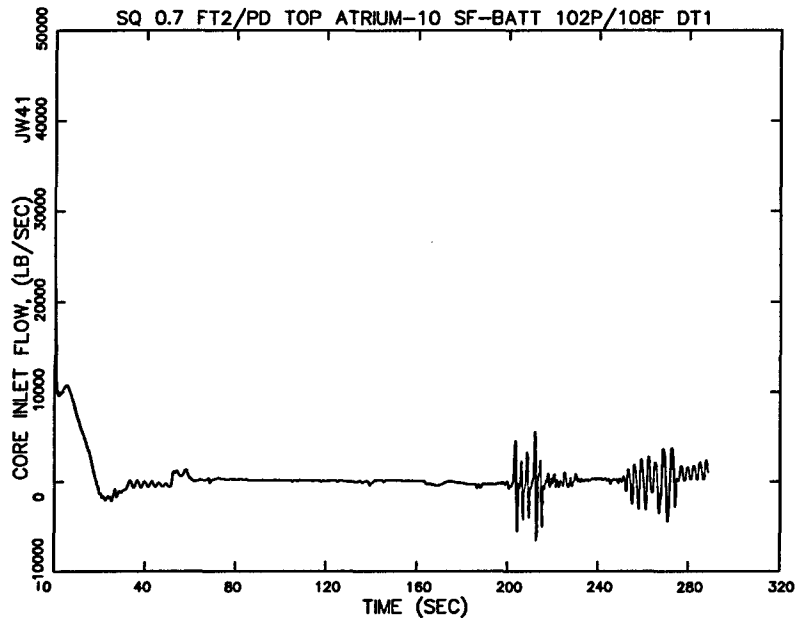


**Figure A.3 0.7 ft<sup>2</sup> PD SF-BATT TOP 108F  
Core Inlet Flow Rate**

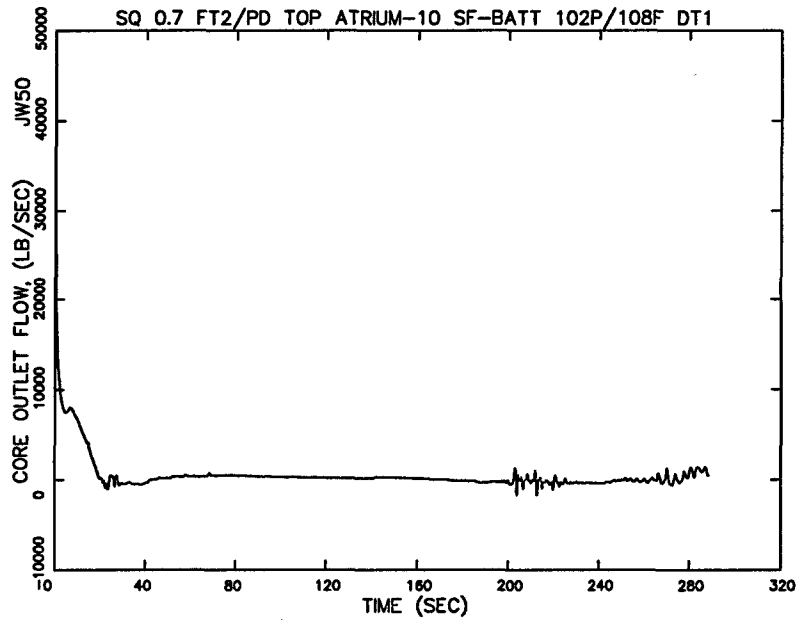


**Figure A.4 0.7 ft<sup>2</sup> PD SF-BATT TOP 108F  
Core Outlet Flow Rate**

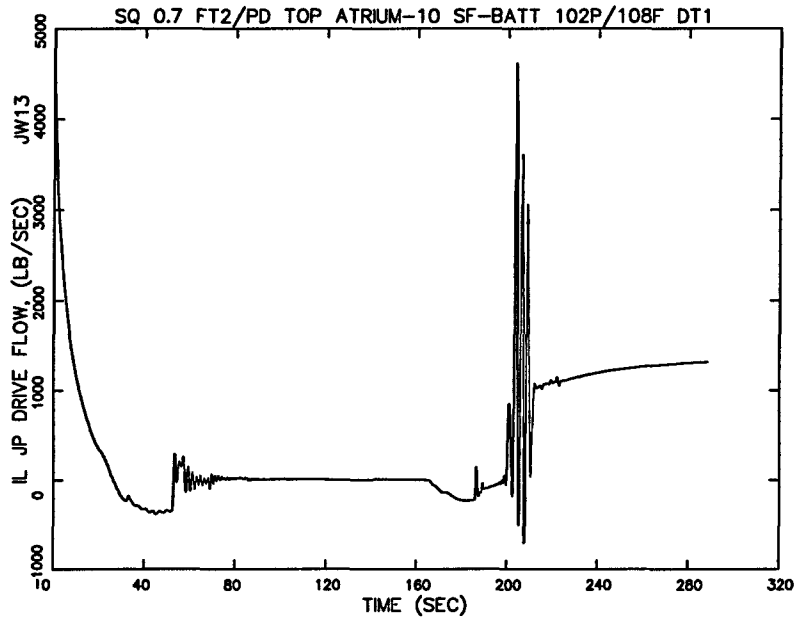


**Figure A.5 0.7 ft<sup>2</sup> PD SF-BATT TOP 108F  
Intact Loop Jet Pump Drive Flow Rate**

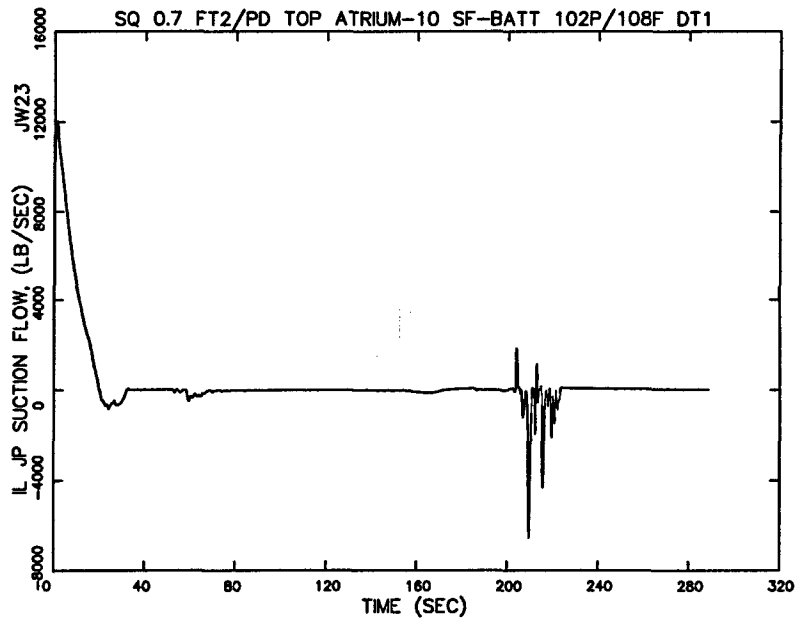


**Figure A.6 0.7 ft<sup>2</sup> PD SF-BATT TOP 108F  
Intact Loop Jet Pump Suction Flow Rate**

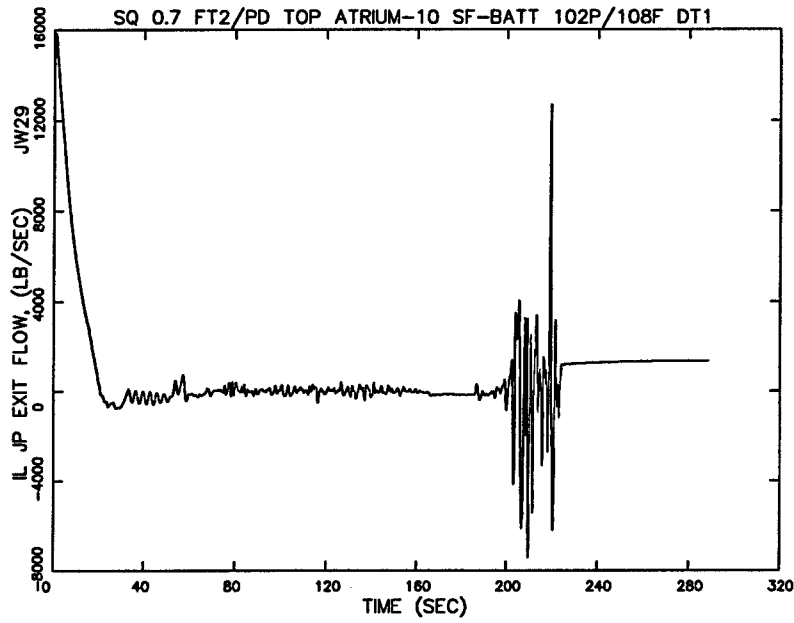


**Figure A.7 0.7 ft<sup>2</sup> PD SF-BATT TOP 108F  
Intact Loop Jet Pump Exit Flow Rate**

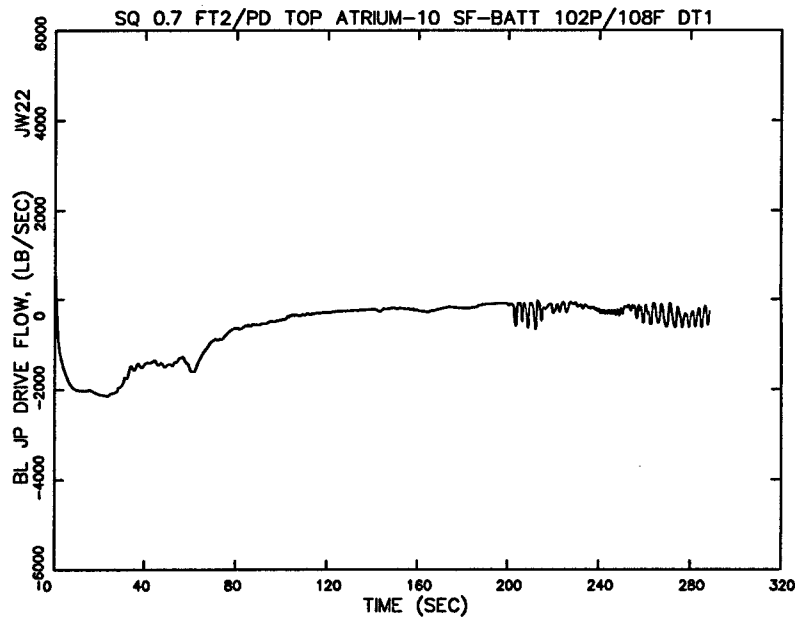


**Figure A.8 0.7 ft<sup>2</sup> PD SF-BATT TOP 108F  
Broken Loop Jet Pump Drive Flow Rate**

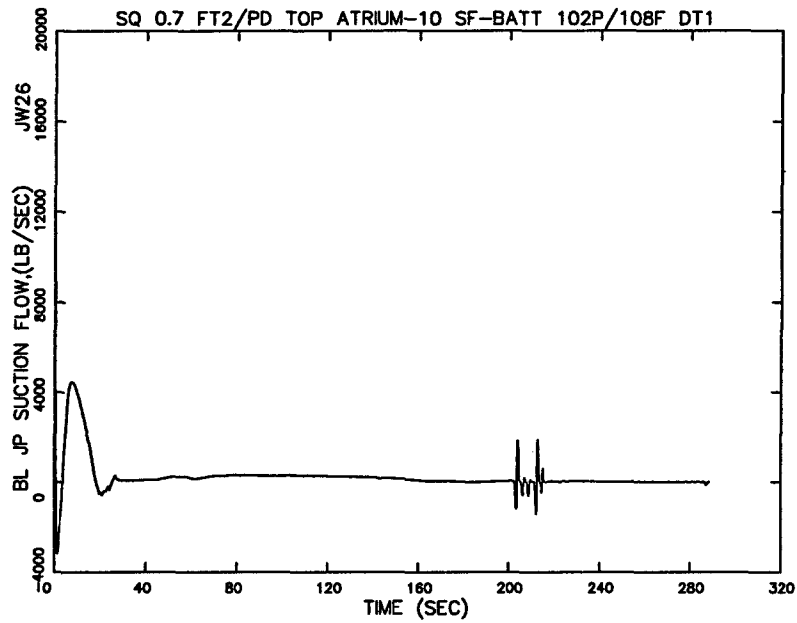


**Figure A.9 0.7 ft<sup>2</sup> PD SF-BATT TOP 108F  
Broken Loop Jet Pump Suction Flow Rate**

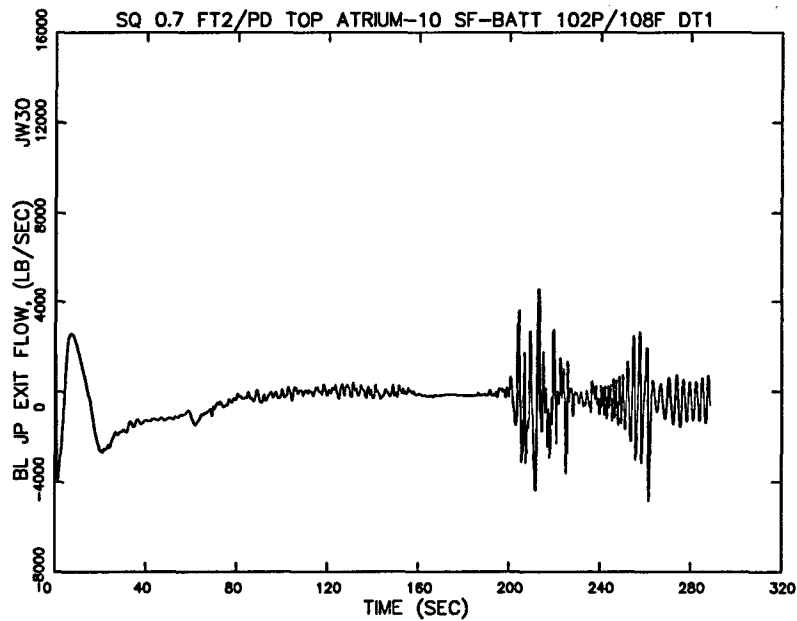


**Figure A.10 0.7 ft<sup>2</sup> PD SF-BATT TOP 108F  
Broken Loop Jet Pump Exit Flow Rate**

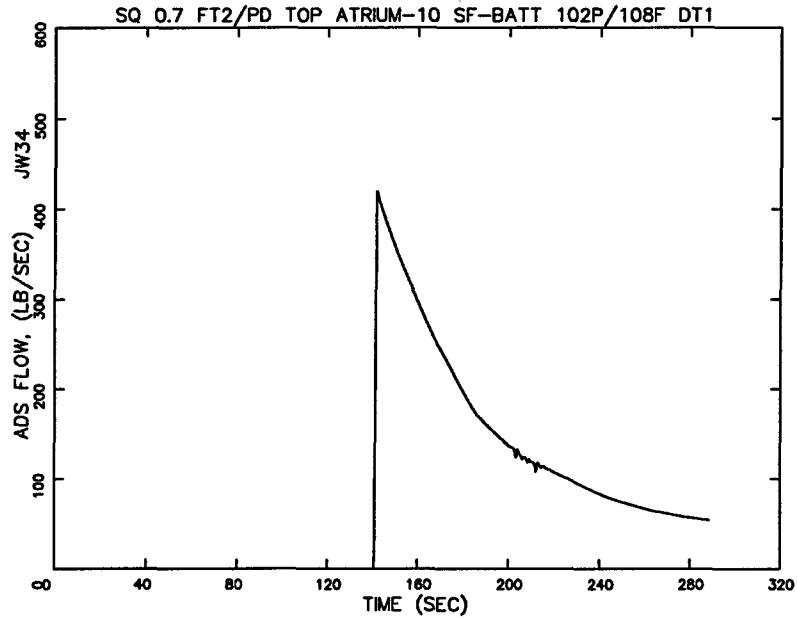


**Figure A.11 0.7 ft<sup>2</sup> PD SF-BATT TOP 108F  
ADS Flow Rate**

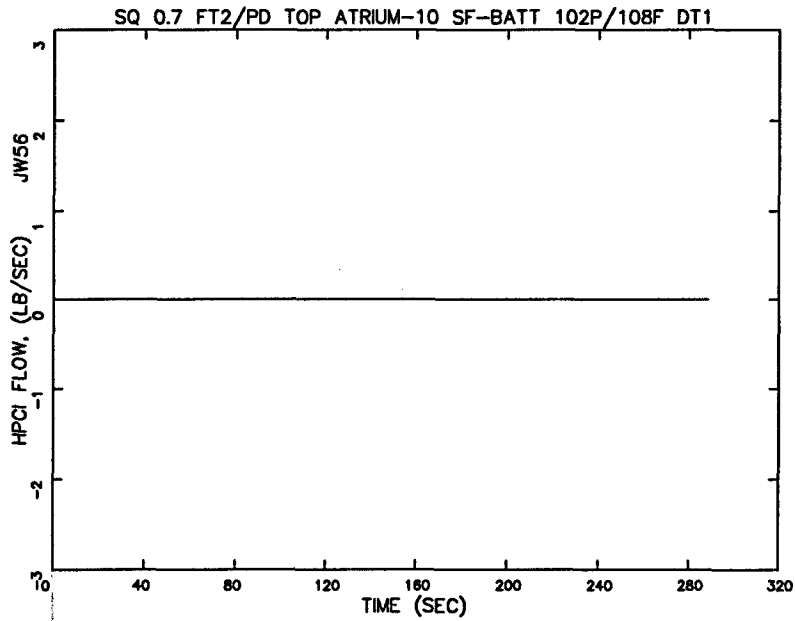


**Figure A.12 0.7 ft<sup>2</sup> PD SF-BATT TOP 108F  
HPCI Flow Rate**

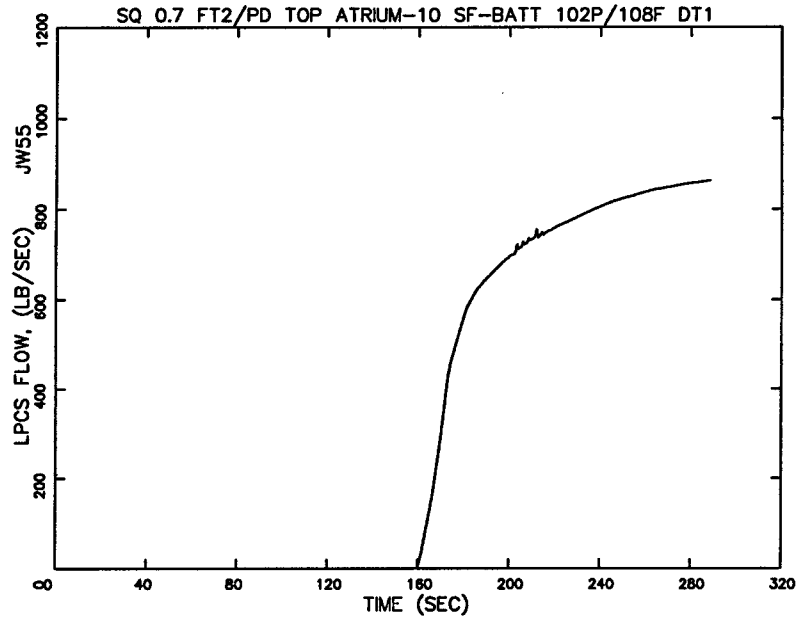


**Figure A.13 0.7 ft<sup>2</sup> PD SF-BATT TOP 108F  
LPCS Flow Rate**

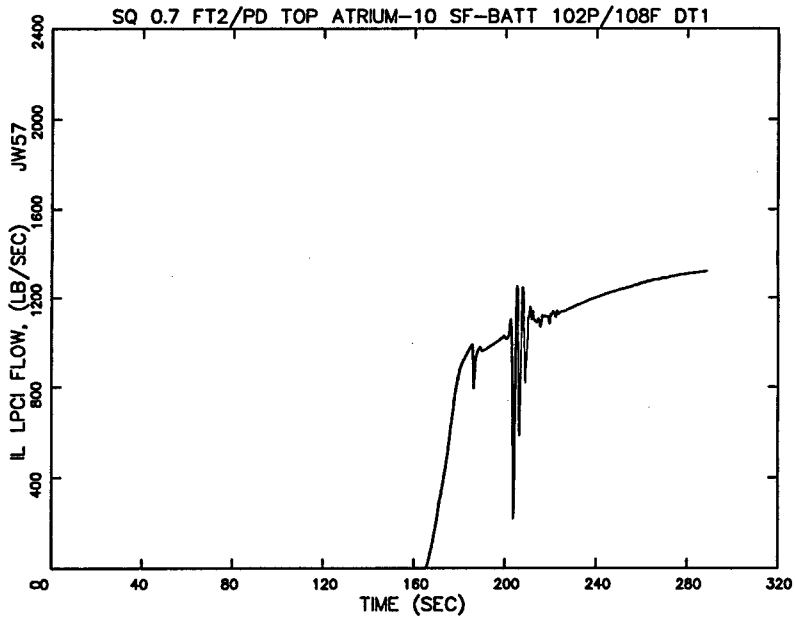


**Figure A.14 0.7 ft<sup>2</sup> PD SF-BATT TOP 108F  
Intact Loop LPCI Flow Rate**

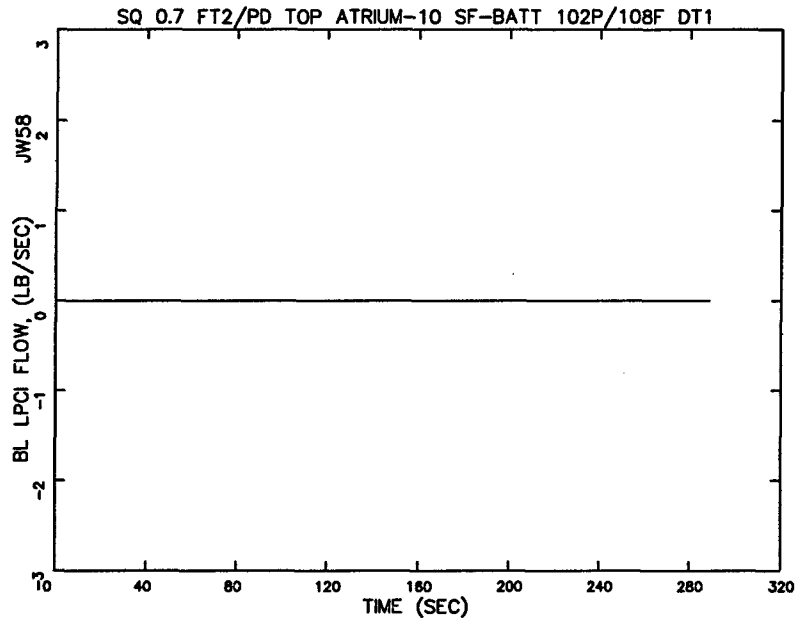


**Figure A.15 0.7 ft<sup>2</sup> PD SF-BATT TOP 108F  
Broken Loop LPCI Flow Rate**

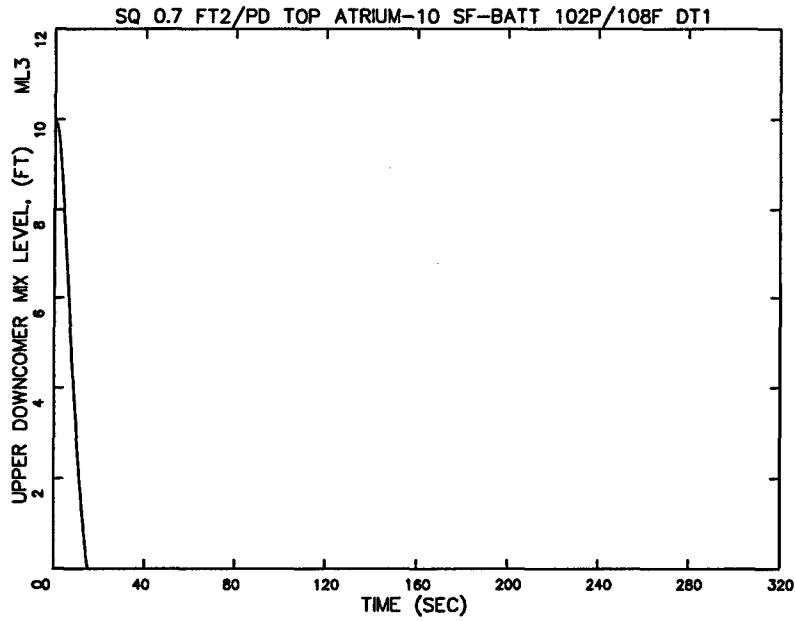


**Figure A.16 0.7 ft<sup>2</sup> PD SF-BATT TOP 108F  
Upper Downcomer Mixture Level**

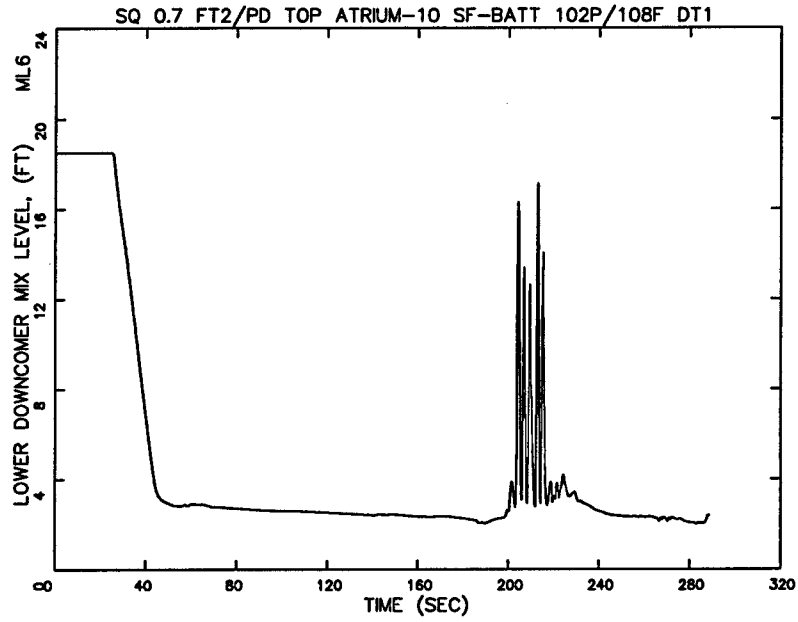


**Figure A.17 0.7 ft<sup>2</sup> PD SF-BATT TOP 108F  
Lower Downcomer Mixture Level**

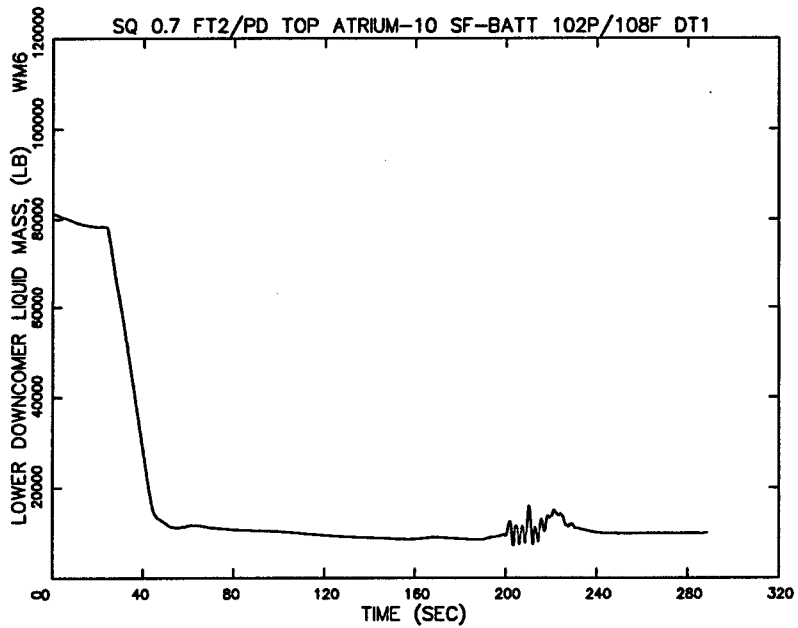


**Figure A.18 0.7 ft<sup>2</sup> PD SF-BATT TOP 108F  
Lower Downcomer Liquid Mass**

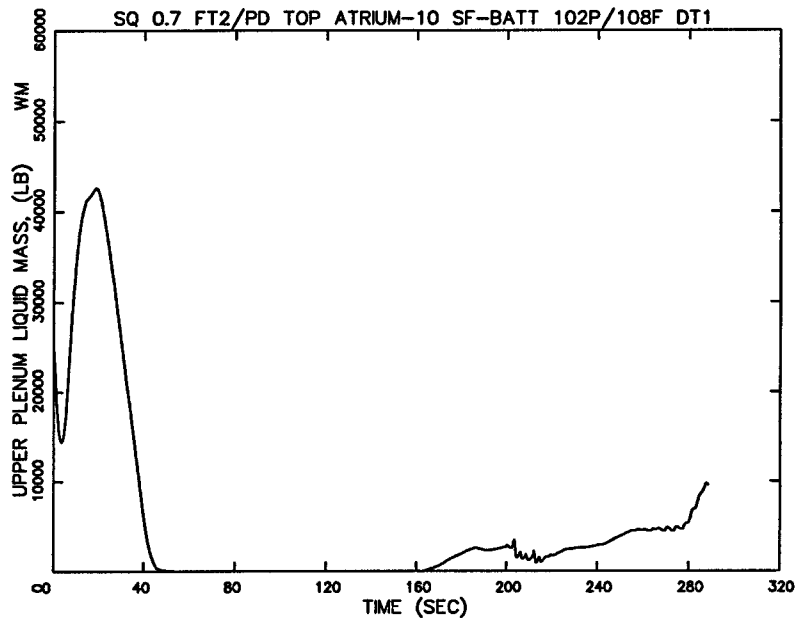


**Figure A.19 0.7 ft<sup>2</sup> PD SF-BATT TOP 108F  
Upper Plenum Liquid Mass**

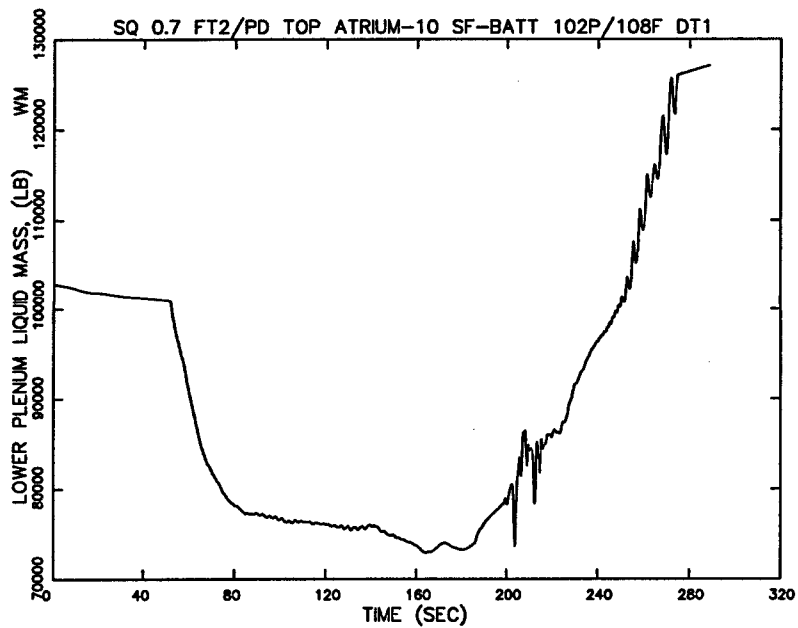


**Figure A.20 0.7 ft<sup>2</sup> PD SF-BATT TOP 108F  
Lower Plenum Liquid Mass**

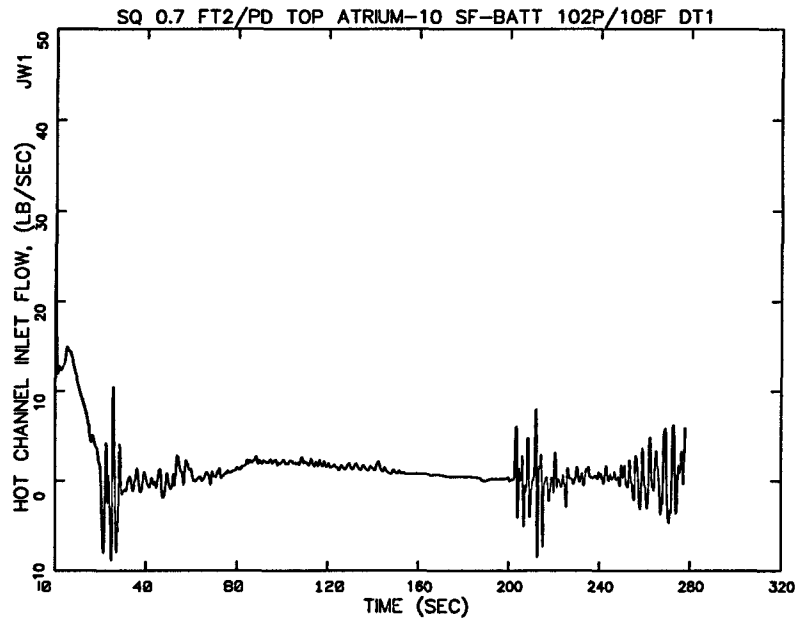


**Figure A.21 0.7 ft<sup>2</sup> PD SF-BATT TOP 108F  
Hot Channel Inlet Flow Rate**

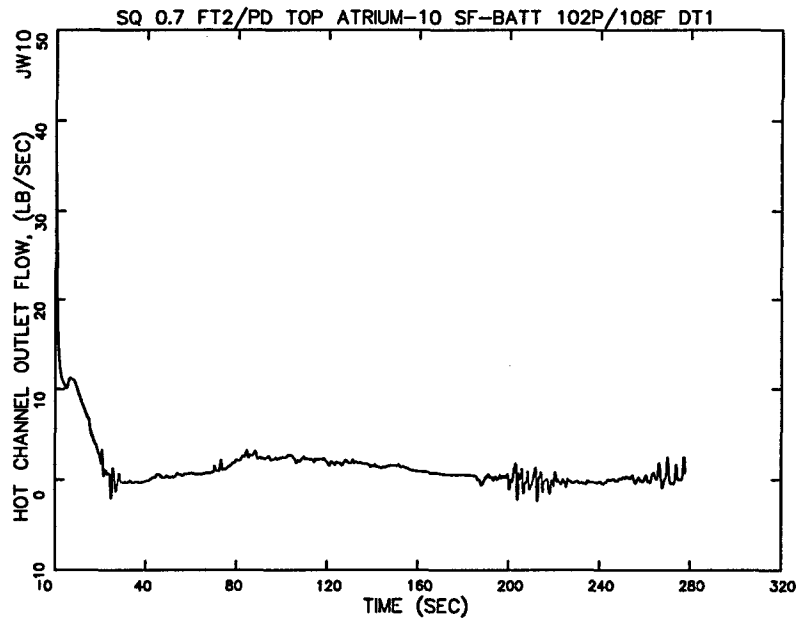


**Figure A.22 0.7 ft<sup>2</sup> PD SF-BATT TOP 108F  
Hot Channel Outlet Flow Rate**

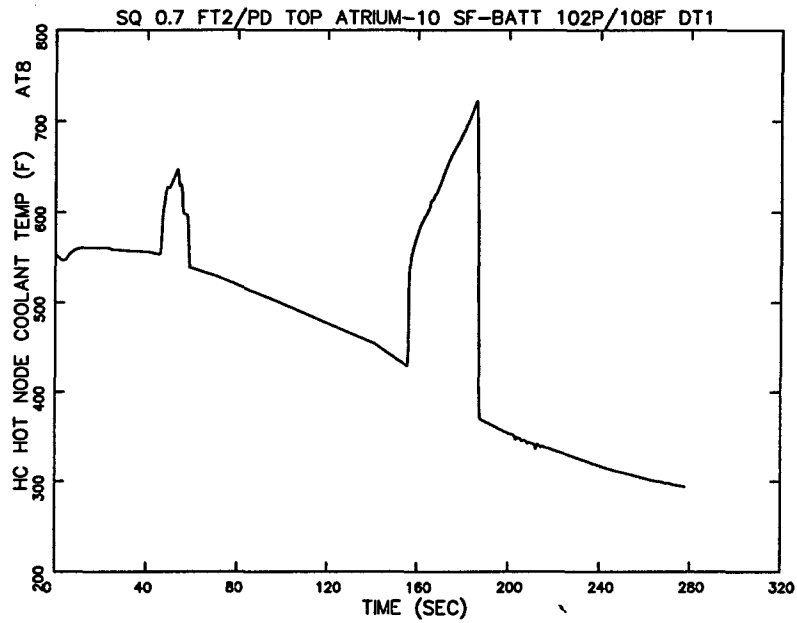


**Figure A.23 0.7 ft<sup>2</sup> PD SF-BATT TOP 108F  
Hot Channel Coolant Temperature at the Limiting Node**

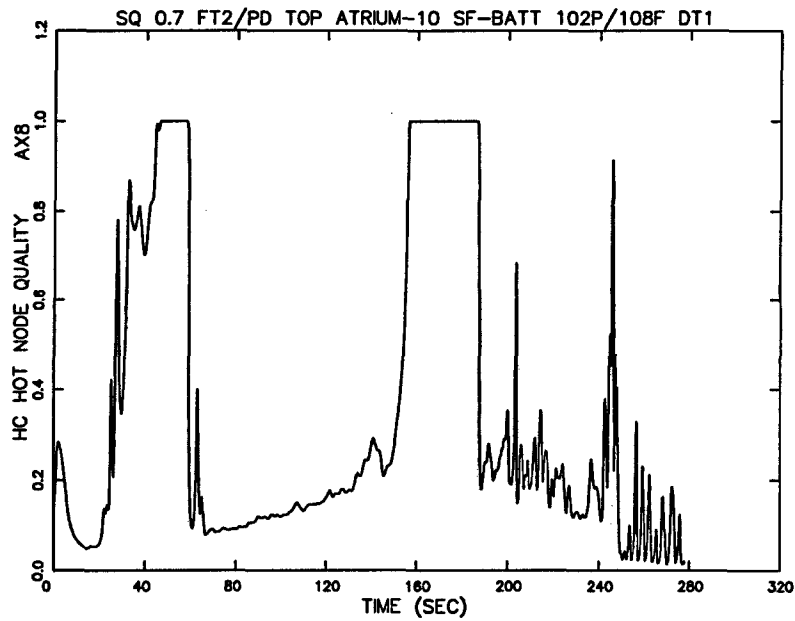


**Figure A.24 0.7 ft<sup>2</sup> PD SF-BATT TOP 108F  
Hot Channel Quality at the Limiting Node**

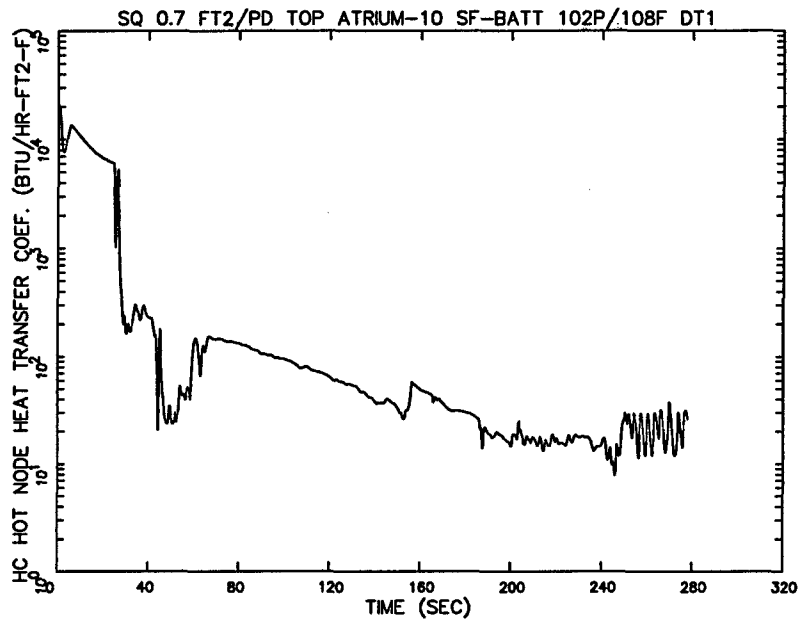


**Figure A.25 0.7 ft<sup>2</sup> PD SF-BATT TOP 108F  
Hot Channel Heat Transfer Coeff. at the Limiting Node**

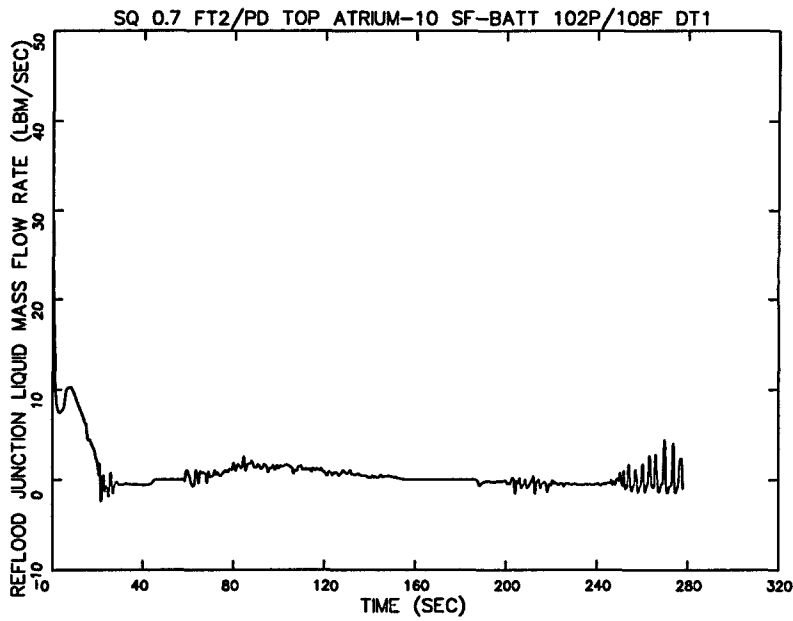


**Figure A.26 0.7 ft<sup>2</sup> PD SF-BATT TOP 108F  
Hot Channel Reflood Junction Liquid Mass Flow Rate**

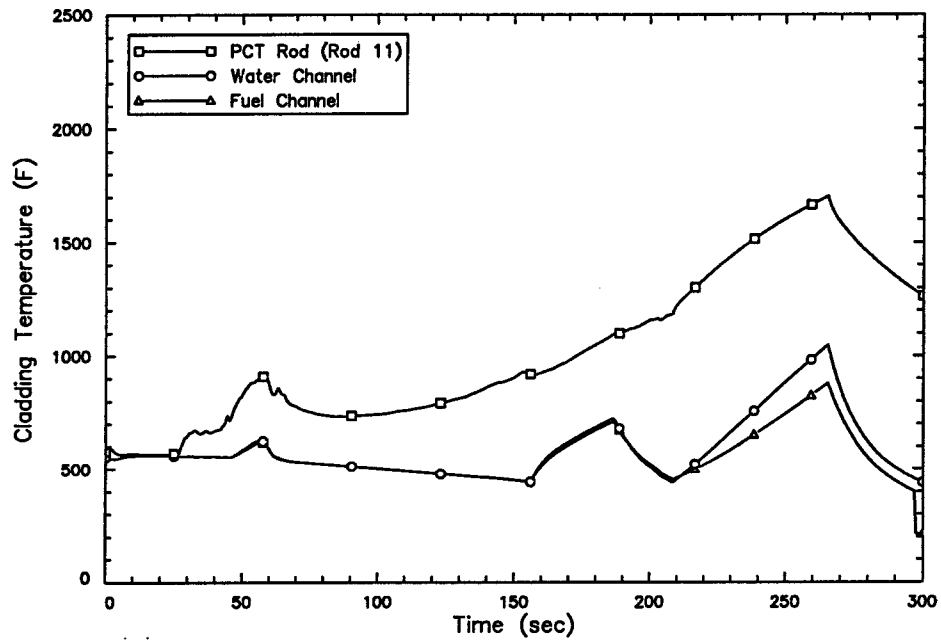


**Figure A.27 0.7 ft<sup>2</sup> PD SF-BATT TOP 108F  
Cladding Temperatures**

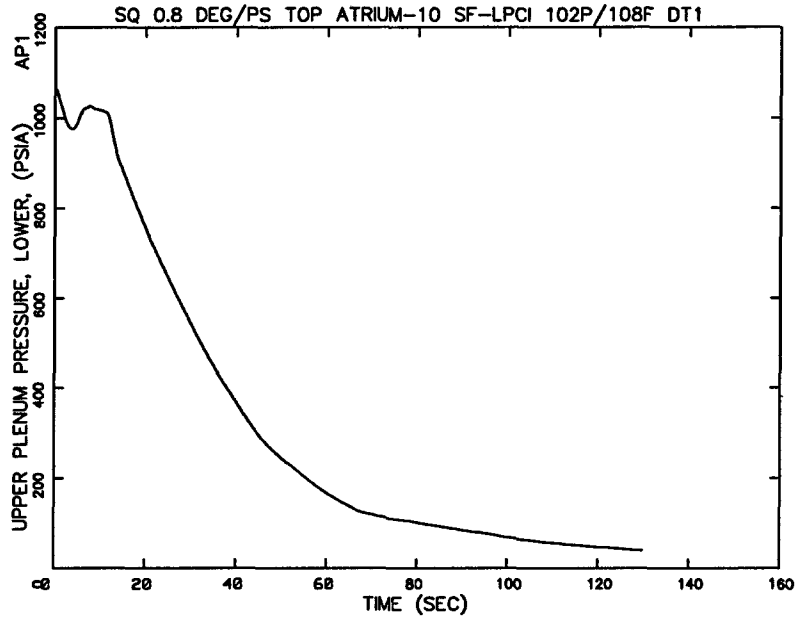


**Figure A.28 0.8 DEG PS SF-LPCI TOP 108F  
Upper Plenum Pressure (Lower)**

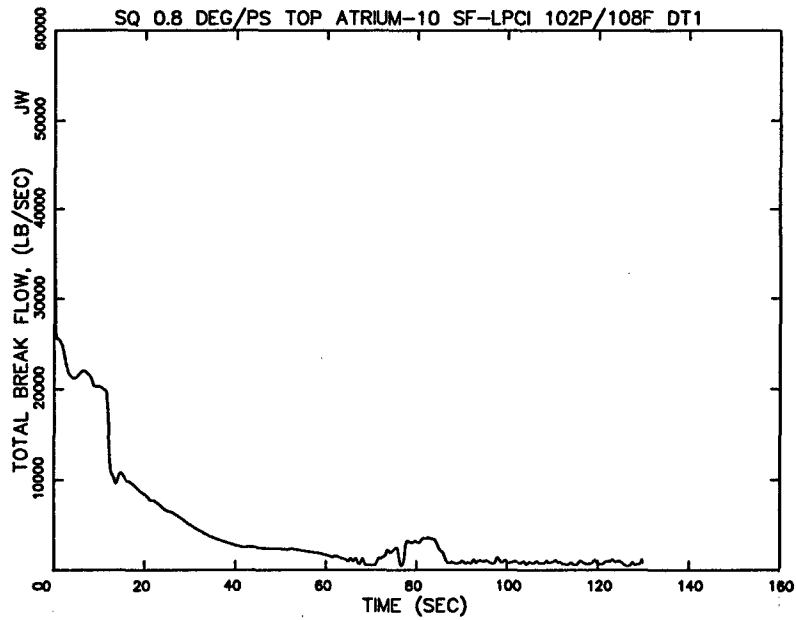


**Figure A.29 0.8 DEG PS SF-LPCI TOP 108F  
Total Break Flow Rate**

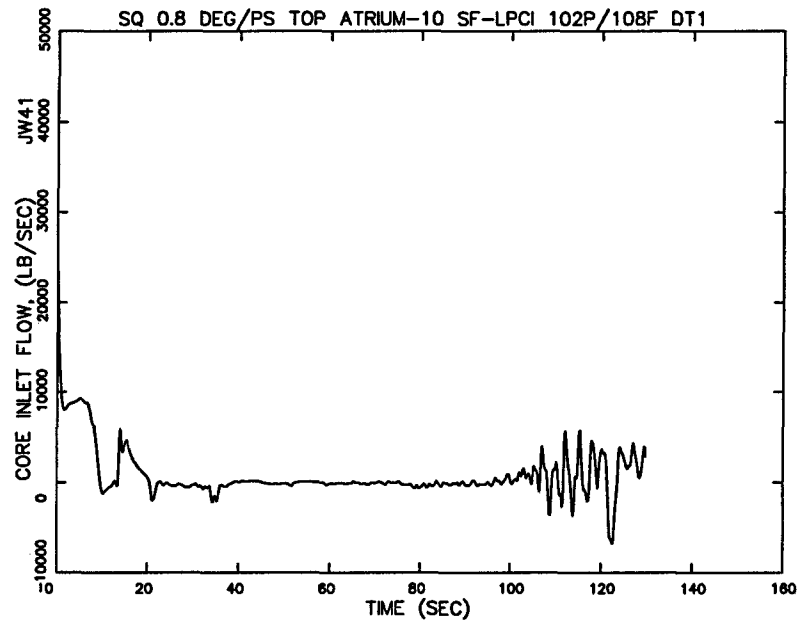


**Figure A.30 0.8 DEG PS SF-LPCI TOP 108F  
Core Inlet Flow Rate**

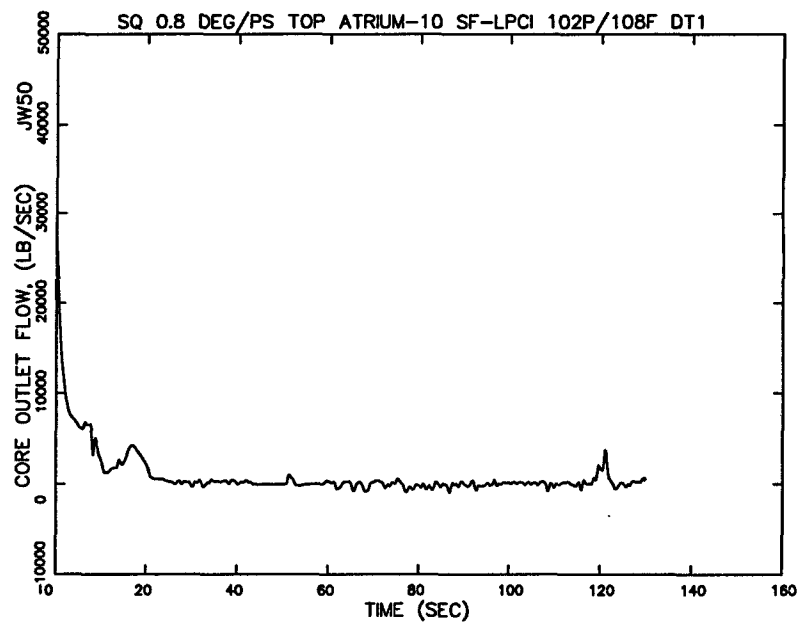


**Figure A.31 0.8 DEG PS SF-LPCI TOP 108F  
Core Outlet Flow Rate**

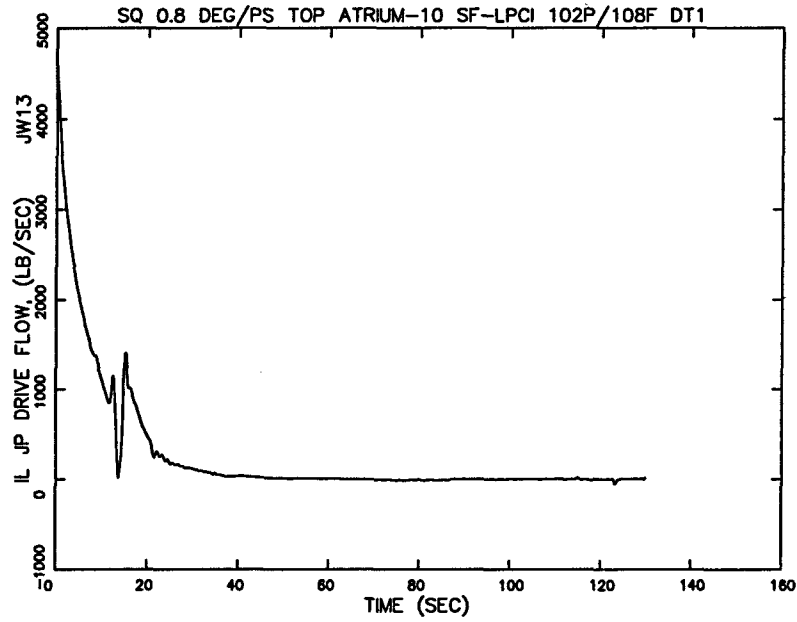


**Figure A.32 0.8 DEG PS SF-LPCI TOP 108F  
Intact Loop Jet Pump Drive Flow Rate**

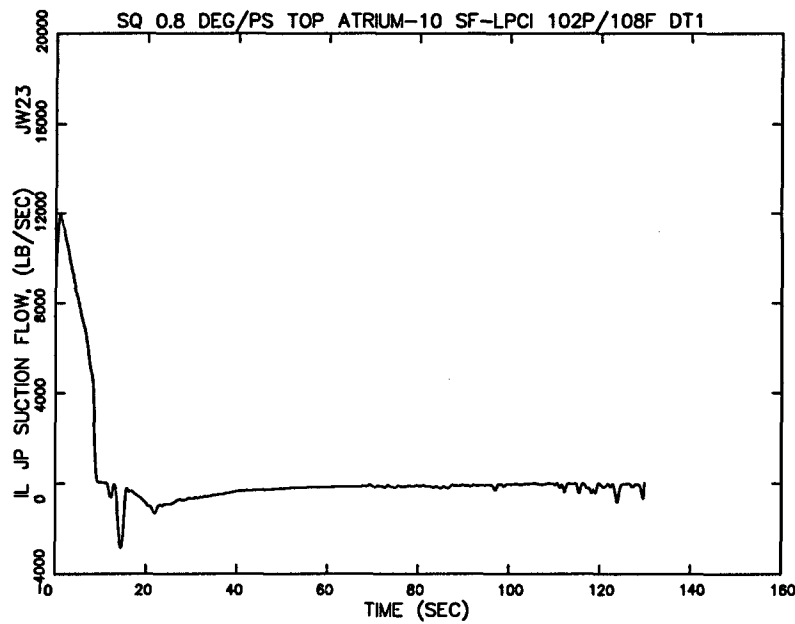


**Figure A.33 0.8 DEG PS SF-LPCI TOP 108F  
Intact Loop Jet Pump Suction Flow Rate**

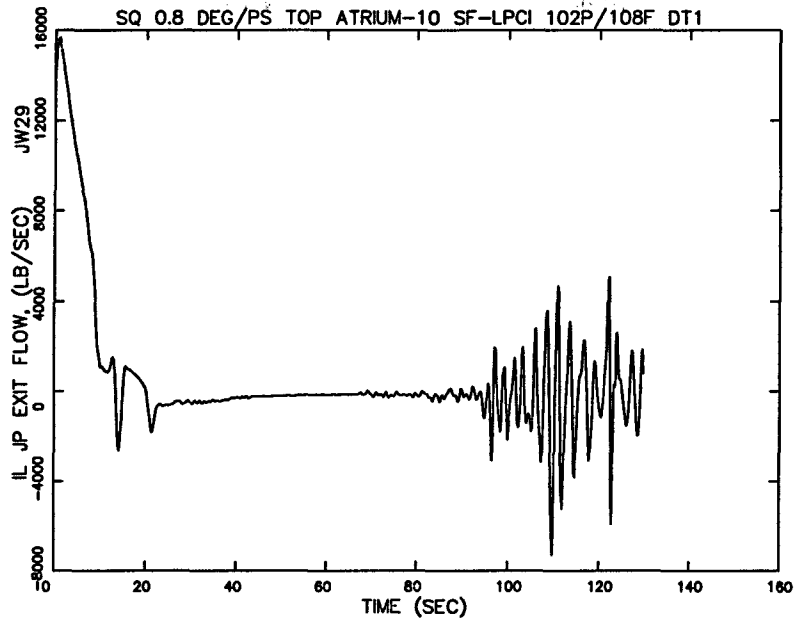


**Figure A.34 0.8 DEG PS SF-LPCI TOP 108F  
Intact Loop Jet Pump Exit Flow Rate**

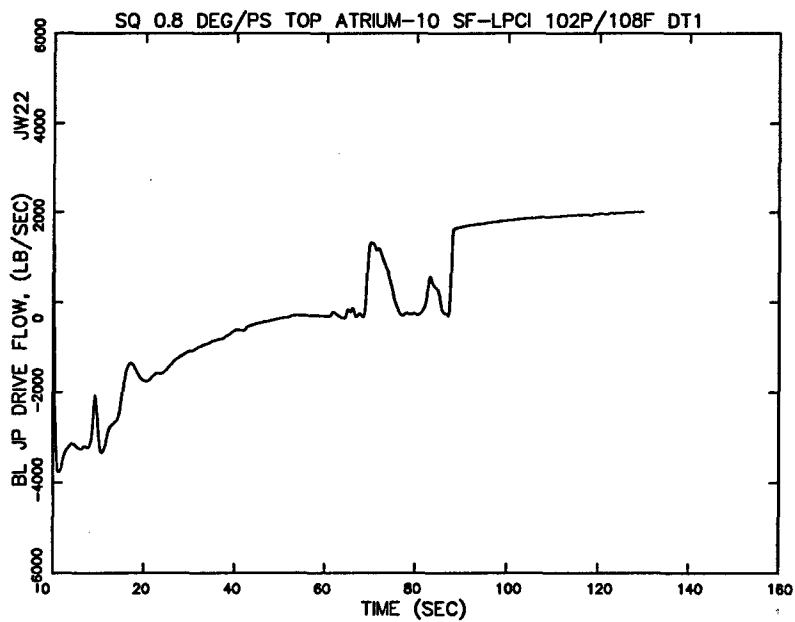


**Figure A.35 0.8 DEG PS SF-LPCI TOP 108F  
Broken Loop Jet Pump Drive Flow Rate**

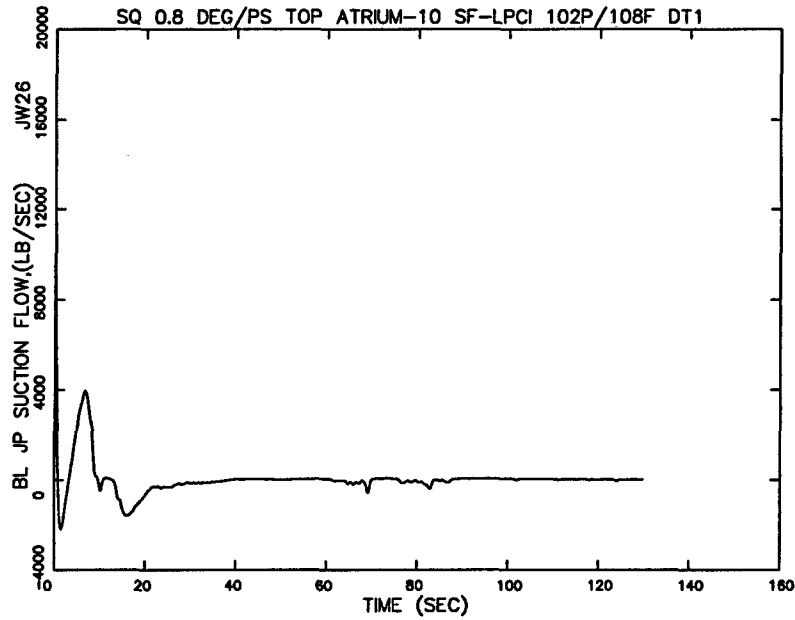


**Figure A.36 0.8 DEG PS SF-LPCI TOP 108F  
Broken Loop Jet Pump Suction Flow Rate**

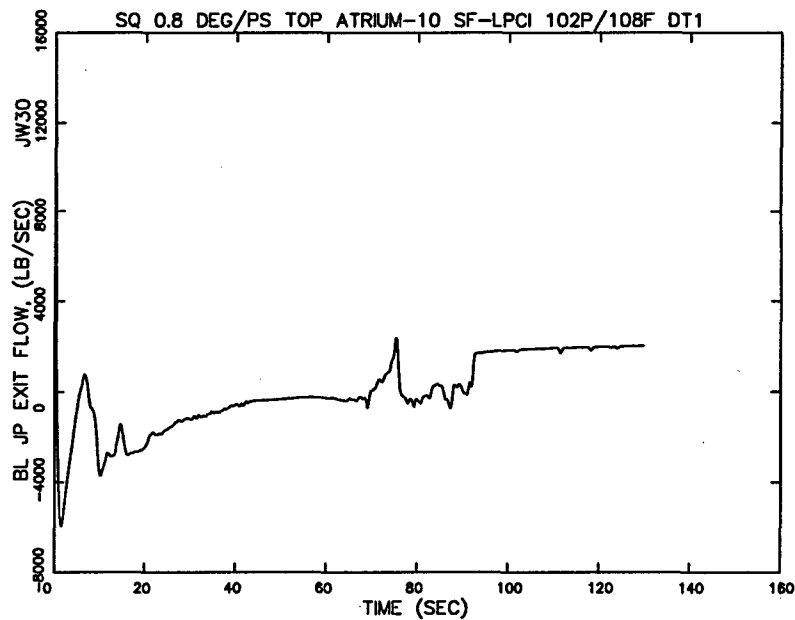


**Figure A.37 0.8 DEG PS SF-LPCI TOP 108F  
Broken Loop Jet Pump Exit Flow Rate**

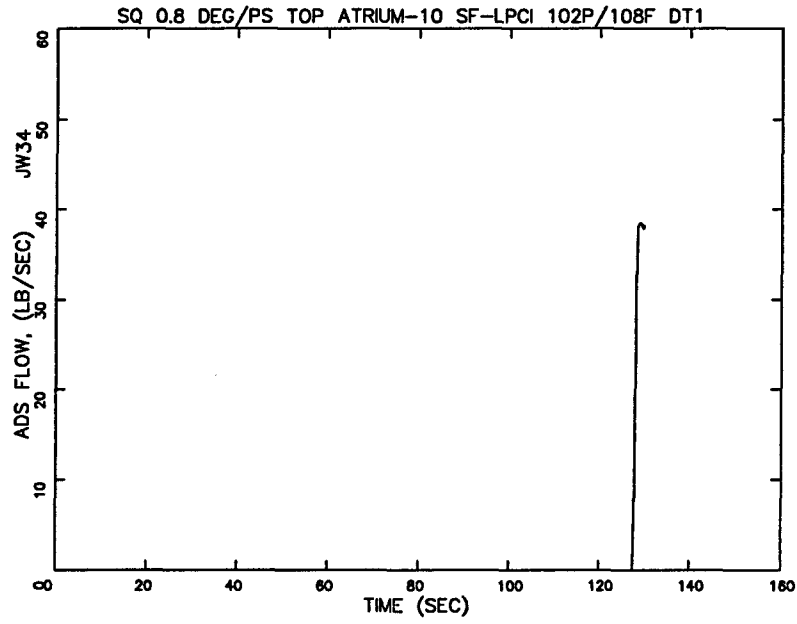


**Figure A.38 0.8 DEG PS SF-LPCI TOP 108F  
ADS Flow Rate**

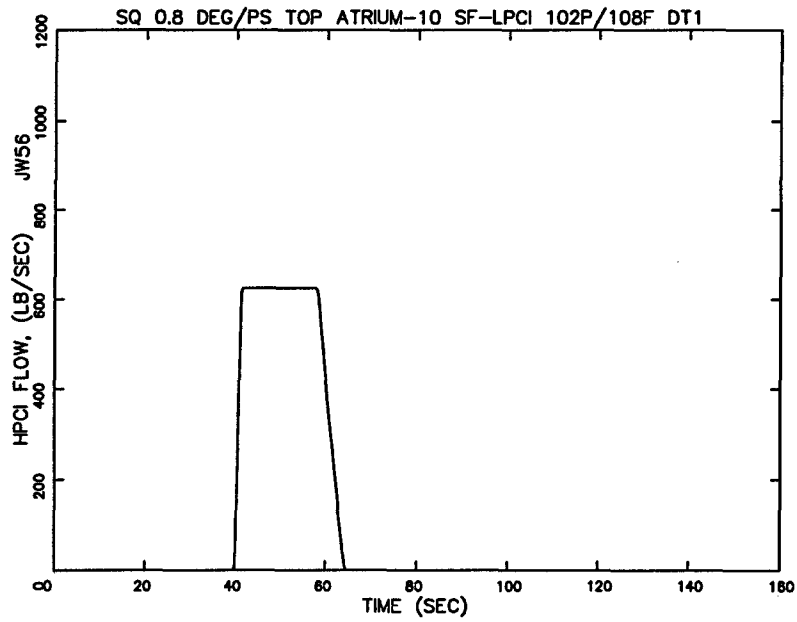


**Figure A.39 0.8 DEG PS SF-LPCI TOP 108F  
HPCI Flow Rate**

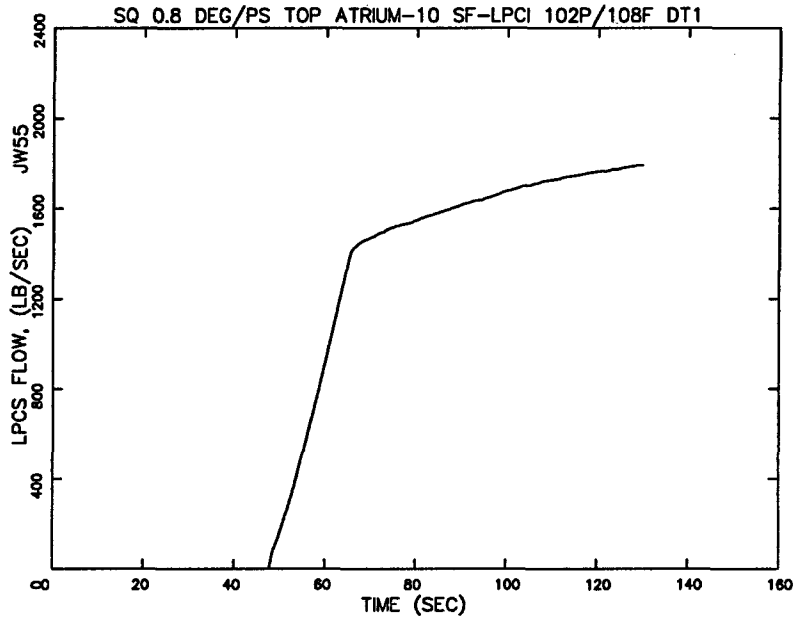


Figure A.40 0.8 DEG PS SF-LPCI TOP 108F  
LPCS Flow Rate

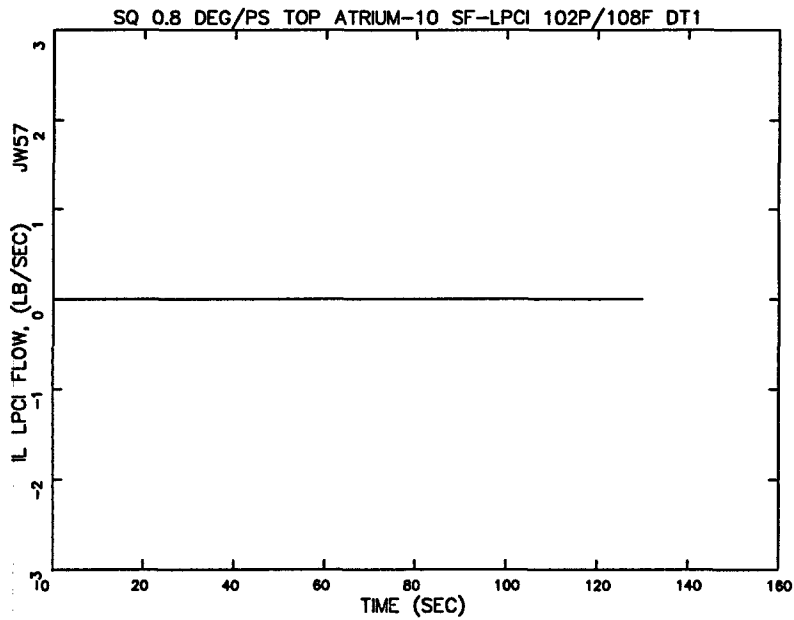
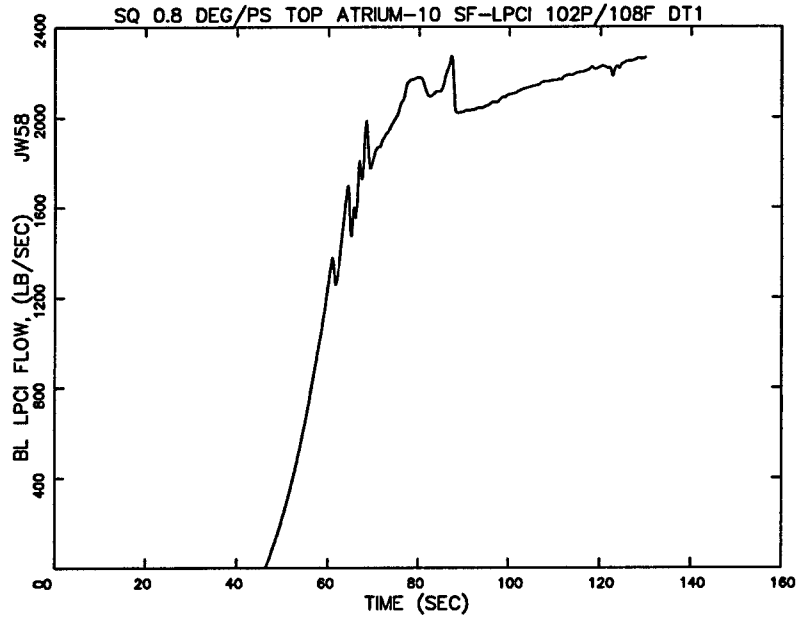
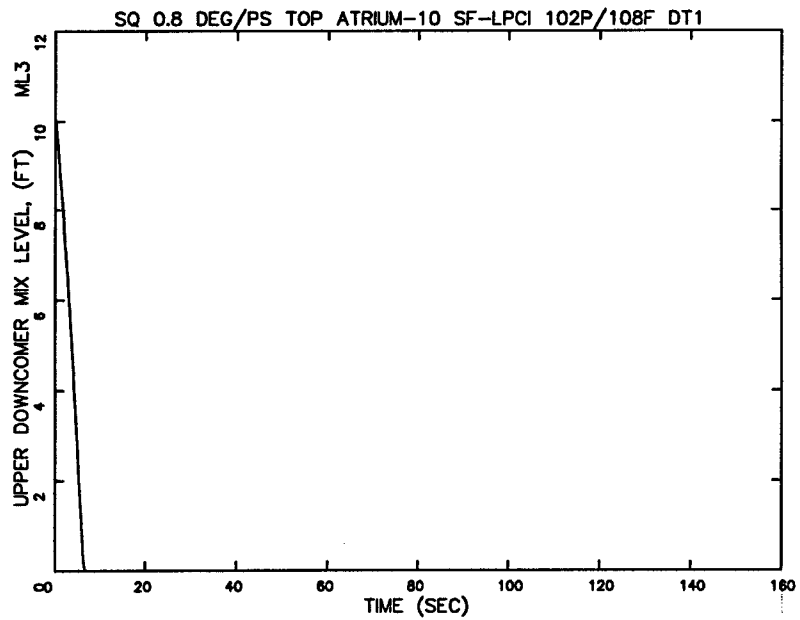


Figure A.41 0.8 DEG PS SF-LPCI TOP 108F  
Intact Loop LPCI Flow Rate



**Figure A.42 0.8 DEG PS SF-LPCI TOP 108F  
Broken Loop LPCI Flow Rate**



**Figure A.43 0.8 DEG PS SF-LPCI TOP 108F  
Upper Downcomer Mixture Level**

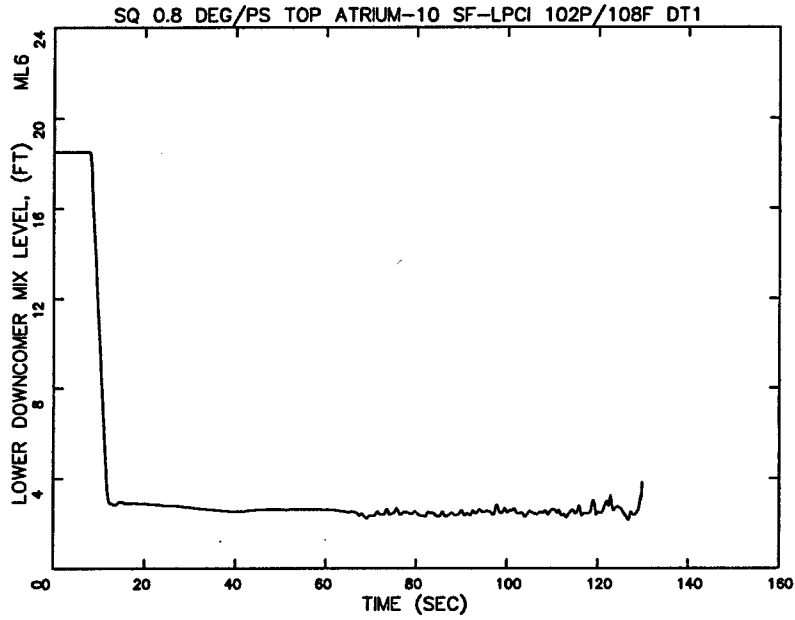


**Figure A.44 0.8 DEG PS SF-LPCI TOP 108F  
Lower Downcomer Mixture Level**

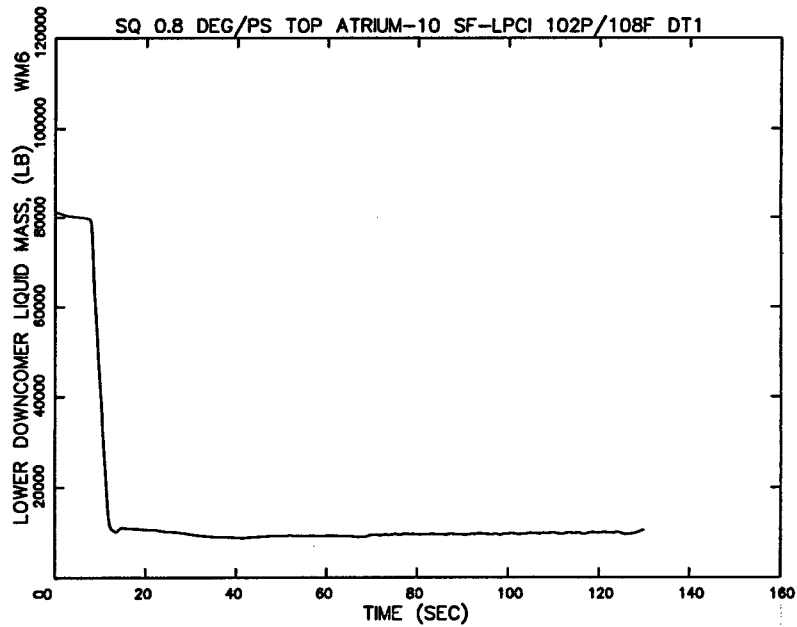


**Figure A.45 0.8 DEG PS SF-LPCI TOP 108F  
Lower Downcomer Liquid Mass**

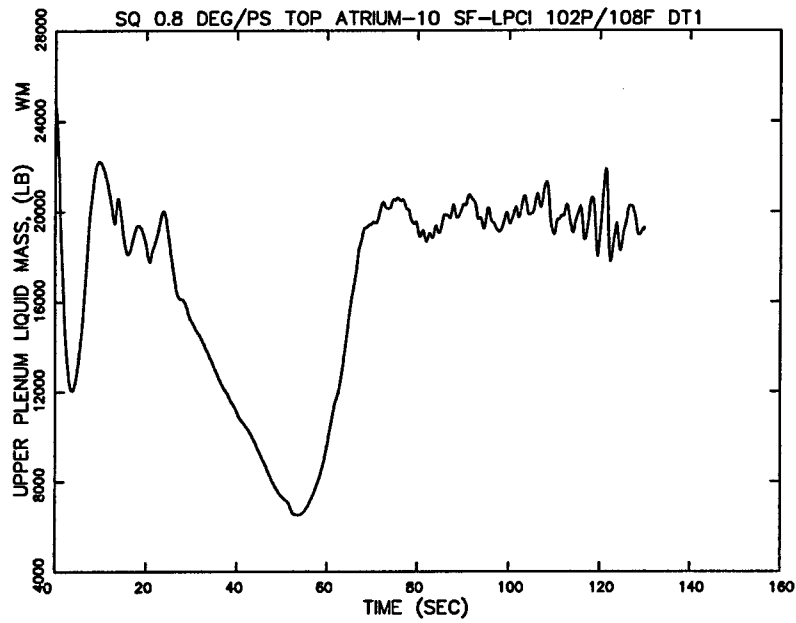


**Figure A.46 0.8 DEG PS SF-LPCI TOP 108F  
Upper Plenum Liquid Mass**

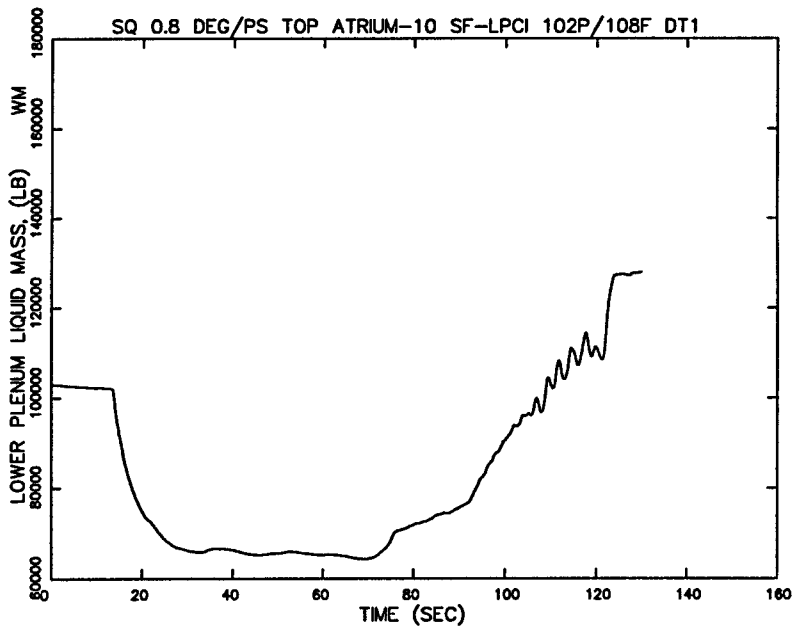


**Figure A.47 0.8 DEG PS SF-LPCI TOP 108F  
Lower Plenum Liquid Mass**

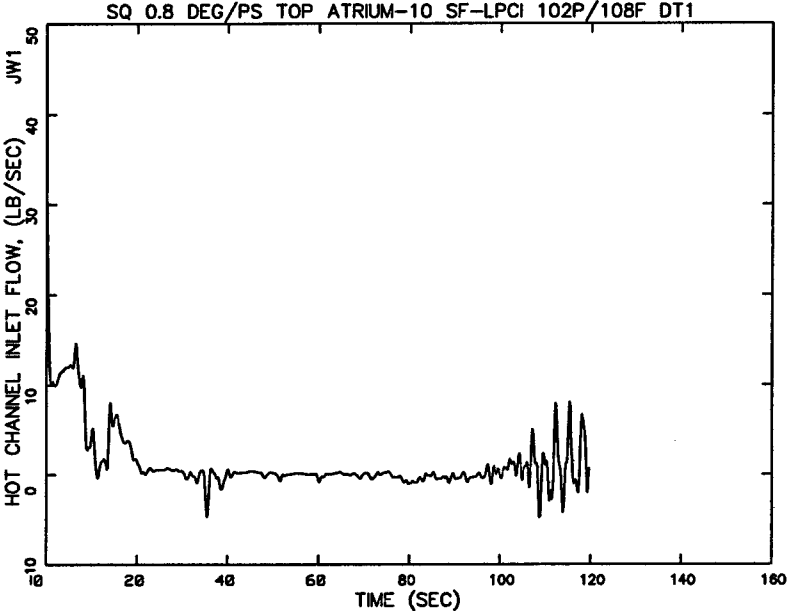


**Figure A.48 0.8 DEG PS SF-LPCI TOP 108F  
Hot Channel Inlet Flow Rate**

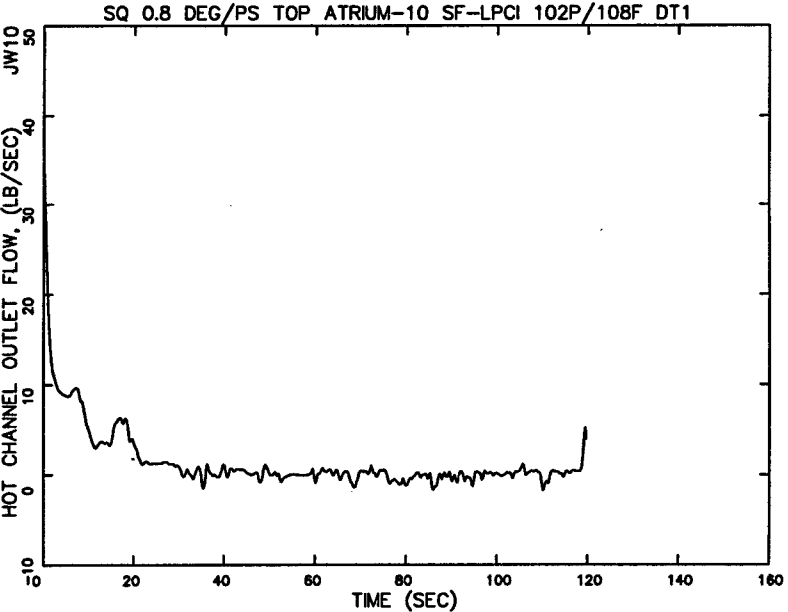


**Figure A.49 0.8 DEG PS SF-LPCI TOP 108F  
Hot Channel Outlet Flow Rate**

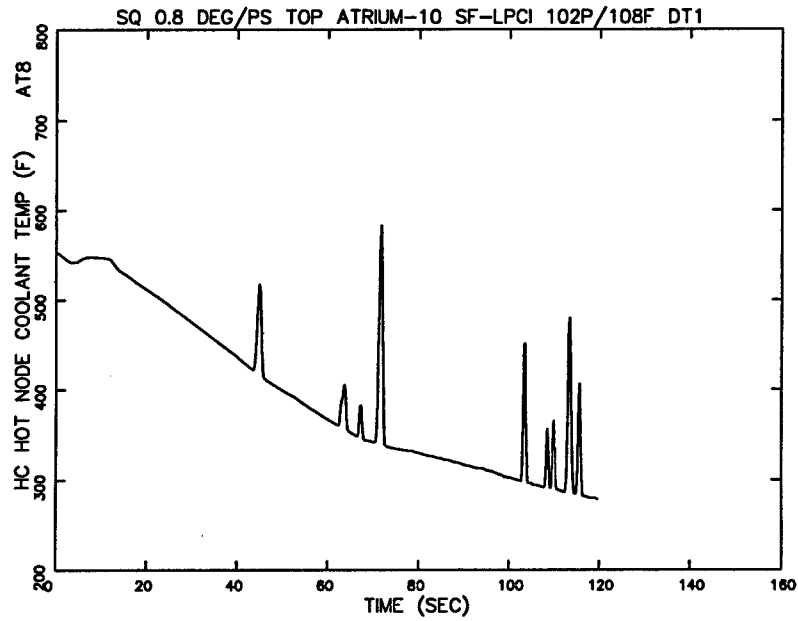


**Figure A.50 0.8 DEG PS SF-LPCI TOP 108F  
Hot Channel Coolant Temperature at the Limiting Node**

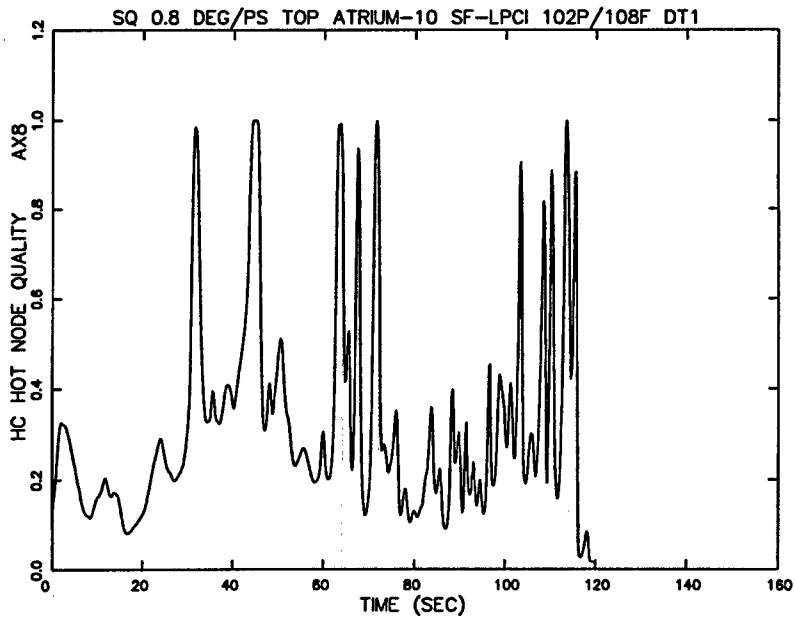


**Figure A.51 0.8 DEG PS SF-LPCI TOP 108F  
Hot Channel Quality at the Limiting Node**

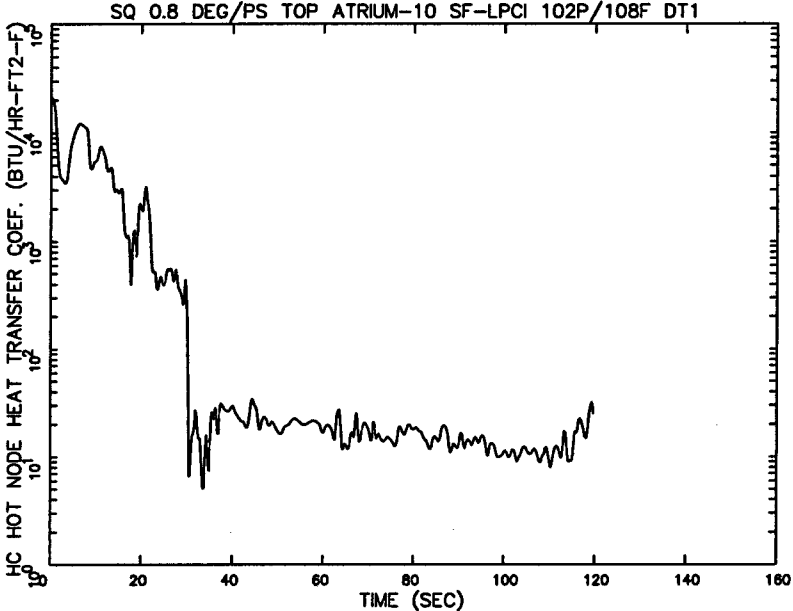


**Figure A.52 0.8 DEG PS SF-LPCI TOP 108F  
Hot Channel Heat Transfer Coeff. at the Limiting Node**

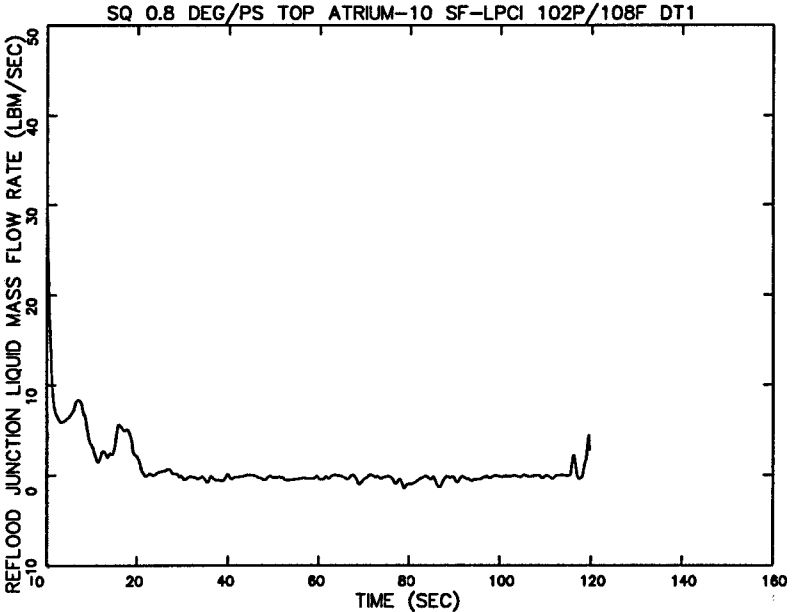


**Figure A.53 0.8 DEG PS SF-LPCI TOP 108F  
Hot Channel Reflood Junction Liquid Mass Flow Rate**

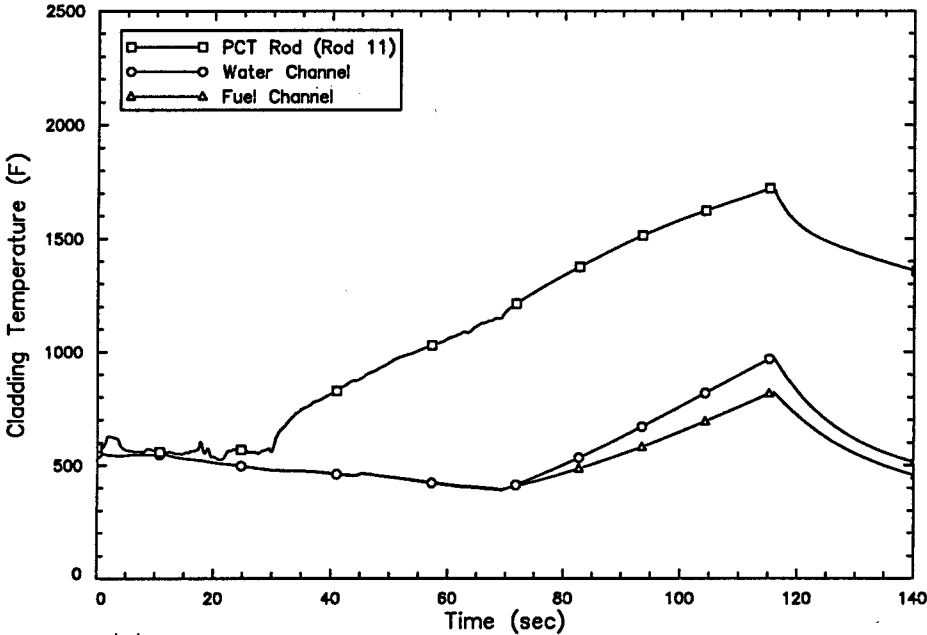


**Figure A.54 0.8 DEG PS SF-LPCI TOP 108F  
Cladding Temperatures**